ผลจากกระบวนการเชื่อมสายเฉพาะที่ในโครงข่ายสุ่มเออร์โดส-เรนยีที่ระบาดแบบปรับตัวได้

นางสาวสุวกัลป์ เพียรกรณีย์

วิทยานิพนธ์นี้เป็นส่วนหนึ่งของการศึกษาตามหลักสูตรปริญญาวิทยาศาสตรดุษฎีบัณฑิต
สาขาวิชาฟิสิกส์ ภาควิชาฟิสิกส์
คณะวิทยาศาสตร์ จุฬาลงกรณ์มหาวิทยาลัย
ปีการศึกษา 2561
ลิขสิทธิ์ของจุฬาลงกรณ์มหาวิทยาลัย

EFFECT OF LOCAL REWIRING IN ADAPTIVE EPIDEMIC ERDŐS-RÉNYI RANDOM NETWORKS

Ms. Suwakan Piankoranee

A Dissertation Submitted in Partial Fulfillment of the Requirements
for the Degree of Doctor of Philosophy Program in Physics
Department of Physics
Faculty of Science
Chulalongkorn University
Academic Year 2018

Thesis Title	EFFECT OF LOCAL REWIRING IN ADAPTIVE EPIDEMIC ERDŐS-RÉNYI RANDOM NETWORKS
By	Ms. Suwakan Piankoranee
Field of Study	Physics
Thesis Advisor	Associate Professor Surachate Limkumnerd, Ph.D.

Accepted by the Faculty of Science, Chulalongkorn University in Partial Fulfillment of the Requirements for the Doctoral Degree

..... Dean of the Faculty of Science
(Professor Polkit Sangvanich, Ph.D.)

THESIS COMMITTEE

..... Chairman
(Assistant Professor Rattachat Mongkolnavin, Ph.D.)

..... Thesis Advisor
(Associate Professor Surachate Limkumnerd, Ph.D.)

..... Examiner
(Associate Professor Somchai Kiatgamolchai, Ph.D.)

..... Examiner
(Associate Professor Udomsilp Pinsook, Ph.D.)

..... External Examiner
(Assistant Professor Kornkanok Bunwong, Ph.D.)

สุวกัลป์ เพียรกรณีย์ : ผลจากกระบวนการเชื่อมสายเฉพาะที่ในโครงข่ายสุ่มเออร์โดส-เรนยีที่ระบาดแบบปรับตัวได้. (EFFECT OF LOCAL REWIRING IN ADAPTIVE EPIDEMIC ERDŐS-RÉNYI RANDOM NETWORKS) อ.ที่ปรึกษา : รศ.ดร.สุรเชษฐ์ หลิมกำเนิด, 76 หน้า.

เครือข่ายการแพร่ระบาดแบบดัดแปลงประกอบด้วยสองกระบวนการหลัก ได้แก่ (1) กระบวนการติดเชื้อ-หายป่วย ซึ่งเป็นกระบวนการที่เปลี่ยนสถานะสุขภาพของโหนด และ (2) กระบวนการเชื่อมสายใหม่ซึ่งเป็นกระบวนการที่เปลี่ยนแปลงโครงสร้างของเครือข่าย ในช่วงสองทศวรรษที่ผ่านมา แบบจำลองโรคระบาดในเครือข่ายดัดแปลงได้รับความสนใจอย่างมาก เนื่องจากความเข้าใจในพลวัตระหว่างสองกระบวนการนี้จะเป็นหัวใจสำคัญในการพัฒนาการควบคุมการแพร่ระบาดได้ อย่างไรก็ตามโดยส่วนใหญ่ในแบบจำลองเหล่านี้ กระบวนการเชื่อมสายใหม่อยู่บนพื้นฐานของข้อมูลในระดับครอบคลุมทั้งเครือข่าย นั่นคือ แต่ละคนรู้สถานะสุขภาพของทุกคนในเครือข่าย แต่ทว่าหลักการนี้ไม่สมจริงในกรณีเครือข่ายขนาดใหญ่ วิทยานิพนธ์นี้มีจุดมุ่งหมายที่จะนำเสนอวิธีการเชื่อมสายที่สามารถปฏิบัติได้จริงในการวางแผนเพื่อควบคุมการแพร่ระบาด โดยได้นำเสนอกระบวนการเชื่อมสายที่อาศัยข้อมูลในวงจำกัดของโหนด โดยเรียกวิธีการแบบดั้งเดิมว่า “การเชื่อมสายใหม่แบบครอบคลุม” และเรียกวิธีการที่นำเสนอใหม่ว่า “การเชื่อมสายใหม่แบบเฉพาะที่” ในงานวิทยานิพนธ์นี้ เราศึกษาแบบจำลองการแพร่ระบาดแบบ SIS โดย S เป็นกลุ่มเสี่ยงต่อการติดเชื้อ และ I เป็นกลุ่มติดเชื้อ บนเครือข่ายแบบดัดแปลงสำหรับกระบวนการเชื่อมสายใหม่แบบครอบคลุมและแบบเฉพาะที่ เราพบว่าเครือข่ายที่มีการเชื่อมสายเฉพาะที่ มีโอกาสน้อยกว่าในการป้องกันการระบาดเมื่อเทียบกับเครือข่ายที่มีการเชื่อมสายครอบคลุม อย่างไรก็ตาม จากผลการจำลองเครือข่ายด้วยมอนติคาร์โลจลน์ได้แสดงให้เห็นว่ามีการซ้อนทับกันของเฟสระหว่างกระบวนการเชื่อมสายทั้งสองแบบ ซึ่งหมายความว่าด้วยข้อมูลที่จำกัด เราสามารถทำนายผลลัพธ์ของการแพร่ระบาดเพื่อนำไปสู่การป้องกันอย่างเป็นระบบได้

ภาควิชา ฟิสิกส์ ..... ลายมือชื่อนิสิต .....

สาขาวิชา ฟิสิกส์ ..... ลายมือชื่อ อ.ที่ปรึกษา .....

ปีการศึกษา 2561 .....

5572870323 : MAJOR PHYSICS
KEYWORDS : ERDŐS-RÉNYI RANDOM NETWORKS / SIS EPIDEMICS / ADAPTIVE NETWORKS / LOCAL REWIRING

SUWAKAN PIANKORANEE : EFFECT OF LOCAL REWIRING IN ADAPTIVE EPIDEMIC ERDŐS-RÉNYI RANDOM NETWORKS. ADVISOR : ASSOC.PROF. SURACHATE LIMKUMNERD, Ph.D., 76 pp.

Adaptive epidemic network is driven by two main processes, (1) infection-recovery process that changes the states of the nodes, and (2) rewiring process that modifies the topology of the network. In the past two decades, epidemic models on adaptive networks have gained interests because understanding the dynamics between these two processes can be key to improving control of diseases. However, in most of these models, the rewiring mechanism is based on information known globally, i.e., everyone knows the health status of all others in the network. This concept is not practical in real life for large network. This dissertation aims to provide a more realistic rewiring model for epidemic-control strategy. We propose a method where the decision of an individual is based on its local information. We call the original rewiring method *global rewiring* and ours *local rewiring*. In this dissertation, we investigate a susceptible-infected-susceptible (SIS) epidemic model on adaptive networks for global and local rewirings. Here we find that local rewiring networks have less chance to prevent disease spreading than global rewiring networks because of limited local information. However, using kinetic Monte Carlo simulations, our results show that there are phase overlaps between both rewiring methods. This means that under a certain circumstance, even with limited local information, we can predict outcomes of an epidemic for systematic interventions.

Department : Physics ..... Student's Signature .....

Field of Study : Physics ..... Advisor's Signature .....

Academic Year : 2018 .....

Acknowledgements

First and foremost, I would like to express my sincere gratitude to my advisor Assoc. Prof. Dr. Surachate Limkumnerd for his continual encouragement and support, and for providing an enthusiasm environment for this work to take place. It has been an honour to be your first PhD student. Also, I would like to thank to our post doctoral research associate Manit Klawtanong for his great contributions to this dissertation. This dissertation would not have been possible without their friendly guidance and their persistent help throughout my doctoral education.

I would also like to thank to people in our group: Asst. Prof. Dr. Kajornyod Yoodee, Asst. Prof. Dr. Patcha Chatraphorn, Asst. Prof. Dr. Sojiphong Chatraphorn, Dr. Chatchai Srinitiwarawong, Dr. Rangsima Chanphana, and Dr. Thiti Taychatanapat for helpful discussions and suggestions during this work. I have enjoyed many interesting discussions and debates on and off the topic with Boonyaluk Namnuan and Kwanruthai Butsriruk.

I would like to thank to members of my graduate committee, Asst. Prof. Dr. Rattachat Mongkolnavin, Assoc. Prof. Dr. Somchai Kiatgamolchai, Assoc. Prof. Dr. Udomsilp Pinsook, and Asst. Prof. Dr. Kornkanok Bunwong for their time, attention and thoughtful comments.

I am also very grateful to the Semiconductor Physics Research Laboratory (SPRL) for providing and maintaining high-efficiency computer facilities. This work was partially supported by Research Funds from the Extreme Condition Physics Research Laboratory and Physics of Energy Materials Research Unit, and also the 90th Anniversary of Chulalongkorn University, Ratchadaphisek Somphot Fund.

I would like to offer special thanks to Asst. Prof. Dr. Nuttakorn Thubthong for many a relaxing coffee time, including great advise for living.

Finally, I need to thank my family. Firstly, my mom for cooking delicious healthy meals. Second, my dad for everything, always. And, finally, my brother, for being my best friend. I am so grateful to have such a wonderful family. Thank you all.

Contents

page

Chapter **page**

List of Figures

Figure **page**

Figure **page**

Figure **page**

CHAPTER I

Introduction

Epidemic models are very useful to understand the rate at which diseases spread and how to control them. Early epidemic models are based on the homogeneously mixed, where it is assumed that each individual has the same chance to contact with an infected individual [1–5]. Deterministic mathematical models have been used to understand the spread of disease in large and uniform population. In general, however, these deterministic models are not sufficient to consider the stochastic dynamics in finite population. Furthermore, each individual comes into contact only with its network-based neighbours [6–9]. Therefore, the structure of population is modelled as a network, where the node represents an individual and a link represents relation or interaction between individuals.

In early works on network epidemic models, the topology of the network is assumed to be fixed, which is called a static network. However, people may change their social behaviours in response to infection to avoid catching it [10–12]. For example, as SARS epidemic zone is declared, people may attempt to reduce their chances of infection by eliminating contacts with infected individuals which may alter the progression of the disease [13]. Then the coevolution between the topology of the network and the epidemic dynamics has been formed. This brings to the concept of an adaptive network [10,14] where changes to the network structure are occurred in dependence of the dynamic state of the nodes and in turn affect future dynamics of the state.

Gross et al. [10] introduced rewiring mechanism based on removing high-risk contacts between the susceptible and infected nodes, and rewiring with non-

infectious contacts. In this model, the total number of links in the network is conserved. This may be assumed to maintain the functionality of the society. Here, the rewiring mechanism occurs at the global level where every node must know epidemiology status of every other in the network. In reality, however, individuals may have incomplete knowledge about the status of the whole network. More practically, the nodes may know the status of other nodes only within their local areas, for example, neighbourhoods including neighbour one, two, or more links away. To make adaptive networks more realistic, the local knowledge should be taken into account.

This dissertation aims to give more practical rewiring model for epidemic control strategy. We simulate the stochastic processes of two rewiring methods. The first method called "global rewiring" is described by the original one [10], while the second method, proposed by us, is called "local rewiring". The words *global* and *local* are used to described the knowledge about health statuses that a node has about its neighbours. In this dissertation, we investigate adaptive model on Erős-Rényi (ER) random networks [15–18], but the introduced framework may be applied to other network structures such as scale-free network [19, 20] as well.

The scope of this work covers the following objectives. We investigate the susceptible-infected-susceptible (SIS) epidemic model with local rewiring on ER random network. We neglect the effects of natural birth and death because epidemic duration is much shorter than the time scale of the demographic process thus the total number of nodes is constant. Also, the number of links is conserved according to the networks with global rewiring [10]. The effects of local information with various values of neighbouring distances are studied and compared with the effects of global information. Here, the neighbouring distance is not a physical distance, but it is defined through paths of nodes in the network. The dynamical consequences of local rewiring network: endemic state, disease-free state and coexistence of bistable state are observed. In addition, the analytic approach to support our simulation results is provided.

The outline of the dissertation is the following: In chapter II, we give a

glimpse into adaptive epidemic networks. We start with SIS model of disease dynamics in fully mixed population with continuous random variables. Then we present a brief overview of some definitions related to networks used in this dissertation. After that we present SIS model on ER random network. Our assumptions are following: (1) network size is large enough to be simulated on our computer cluster which is up to 10,000 nodes, (2) links are distributed homogeneously in the network, and (3) the degree distribution used in the pair approximation is based on Poisson distribution. In the last section, we explain SIS dynamics on adaptive networks and show prior results as background for our research that will be presented in Chapters III and IV.

In Chapter III, we propose the local rewiring method where rewired links are restricted within a neighbouring area. We then introduce the most commonly used simulation algorithm for stochastic process known as kinetic Monte-Carlo algorithm [21–24]. In this work we propose an alternative analytical approach for calculating the phase transition for the local rewiring method

In chapter IV, we present our numerical results of epidemic networks at different network sizes and epidemic parameters. We study the effects of the local rewiring mechanism on the epidemic spread, investigate how it change the network topology and phase diagram.

Finally, we draw the conclusions of our work and consider what future research is possible in the field of epidemics on adaptive networks in Chapter V.

CHAPTER II

The Adaptive Epidemic Networks

2.1 Compartmental SIS model

One of the standard approaches to study epidemiology is through what are traditionally called compartmental models [1–5]. The population is divided into different compartments based on the epidemiological status of each individual. The number of compartments and the ways in which individuals move from one compartment to another depends on the nature of the disease being modelled. In the case of susceptible-infected-susceptible (SIS) model, there are two compartments, S (susceptible) and I (infected) [8]. Susceptible individuals are healthy ones who are susceptible to the disease if they come into contact with infected individuals who are currently infected and able to spread the disease to susceptible individuals. In this model, the infected becomes susceptible again immediately after recovery. The SIS model assumes that there is no immunity for the disease then the individuals can be infected over again following a cycle $S \to I \to S$. The transition rates from one compartment to another are mathematical expressed as derivatives. In the following, we will introduce the rate equation of each compartment and its solutions.

2.1.1 Mathematical approach to SIS model

Mathematical models can estimate how infectious disease progress to show the consequence of an epidemic. In SIS model there are two possible transitions: (1)

Figure 2.1: This diagram shows transitions between compartments consisting of individuals with the same state in the SIS model. The solid line denotes an infection process and the dashed line denotes a recovery process.

infection, denoted by $S \to I$, and (2) recovery, denoted by $I \to S$ (Fig. 2.1). In the continuous-time limit, $I \to S$ transition occurs at the recovery rate of r. The time an individual spends on average in the infected compartment, an average infectious period, is approximately r^{-1}.

A formula of $S \to I$ transition is more complicated than $I \to S$ depending on the modelling consideration. Here, the mathematical models are as good as the assumption of homogeneous mixing, i.e., every individual has the same probability to make a contact with any other [1, 8]. With this assumption, the larger the number of infected individuals, the higher the probability of transmission of the disease. So the probability that susceptible individuals acquire the disease per unit time is $b\langle k\rangle I/N$, where b is the infection rate per contact and $\langle k\rangle$ is the number of contact with other individuals per unit time [8, 9, 25].

These transitions can be modelled by reaction-diffusion type process where the transition is defined by its reaction rates [26]. The time evolution of the epidemic is described by deterministic rate equations stating that the average change in the number of individuals of each compartment due to interactions is given by the product of the force of infection times the average individuals. Let the number of population be conserved, i.e., $N = S + I$. If N is large, we can treat S and I as continuous variables, and the model is fairly well described by

the following rate equations:

$$\begin{aligned} \frac{dS}{dt} &= -b\langle k\rangle \frac{I}{N} S + rI, \\ \frac{dI}{dt} &= b\langle k\rangle \frac{I}{N} S - rI. \end{aligned} \tag{2.1}$$

These equations rely on the homogeneously mixing approximation which assumes that the susceptible and infected individuals are well mixed and interact with each other at random. In this dissertation, we neglect the effects of natural birth and death because the duration of an epidemic is much shorter than the time scale of the demographic process. At this stage, the disease is also not life threatening.

2.1.2 Basic results of the SIS model

To express the solution of Eq. 2.1 it is often convenient to define variables representing the density of susceptible and infected individuals:

$$s = \frac{S}{N}, \qquad i = \frac{I}{N}.$$

With the normalisation condition $s + i = 1$, Eq. 2.1 reduces to

$$\frac{di}{dt} = b\langle k\rangle i(1-i) - ri = (b\langle k\rangle - r - b\langle k\rangle i)i. \tag{2.2}$$

Here we choose to investigate the dynamic of the infected fraction rather than the susceptible fraction because the existence of infection describes the epidemic state.

The solution of Eq. 2.2 provides the density of infected individuals as a function of time

$$i = \left(1 - \frac{r}{b\langle k\rangle}\right) \frac{Ce^{(b\langle k\rangle - r)t}}{1 + Ce^{(b\langle k\rangle - r)t}}, \tag{2.3}$$

where the integration constant C is fixed by the initial condition $i_0 = i(t = 0)$ so that

$$C = \frac{i_0}{1 - i_0 - \frac{r}{b\langle k\rangle}}. \tag{2.4}$$

Eq. 2.3 predicts that there are two possible outcomes:

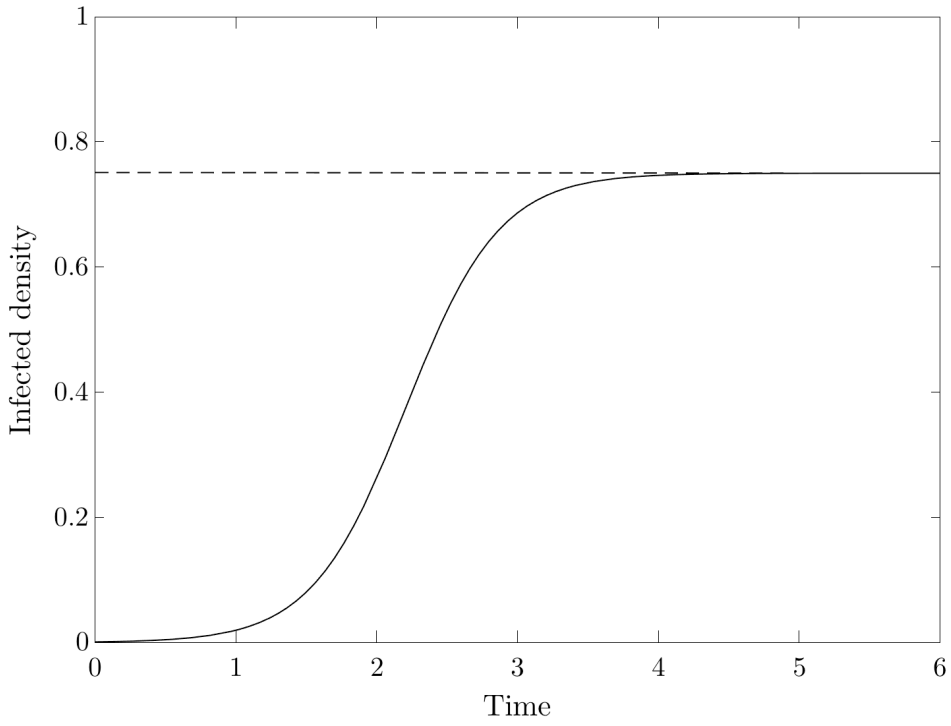

Figure 2.2: The density of infected individuals grows with time following a sigmoid function and tends to constant density at which the rates of infection and recovery are balanced.

- **Endemic state** when $b\langle k\rangle - r > 0$ or $b\langle k\rangle/r > 1$.

  In this condition, the infected fraction i follows a sigmoid function (see Fig. 2.2). At long time, i reaches a constant i_∞ calculated by setting Eq. 2.2 to zero:

  $$i_\infty = 1 - \frac{r}{b\langle k\rangle}. \tag{2.5}$$

  In this state, the rates that individuals are infected and recover from infection are exactly equal. Consequently the infected density does not change with time. This steady state is called *endemic state*.

- **Disease-free state** when $b\langle k\rangle - r < 0$ or $b\langle k\rangle/r < 1$.

  In this condition, i decreases exponentially with time, indicating that the disease will die out eventually. This is because the number of individuals who recovered per unit time is larger than the number of new infected individuals. Therefore at long time, the disease disappears from the population.

From outcomes above, the condition $b\langle k\rangle = r$ indicates a transition between a state in which the disease can spread and one in which it cannot. This transition is called an *epidemic transition* (Fig. 2.3) and the point of the transition is called the *basic reproduction number* or the *basic reproductive ratio* R_0 [27–30],

$$R_0 = \frac{b\langle k\rangle}{r}. \tag{2.6}$$

R_0 is defined as the average number of secondary infections caused by a primary infected individual introduced in a completely susceptible population. If $R_0 > 1$, the epidemic is in the endemic state. If $R_0 < 1$, then the epidemic is in disease-free state. The point $R_0 = 1$ marks the *epidemic threshold* between these two states.

The classical SIS model ignores the fact that individuals come into contact only with their neighbours in the contact network that facilitates the spread of a disease. Classical SIS assumes homogenous mixing, which means that an infected individual can interacts other individuals with the probability depending on their populations. It means that an infected individual typically infects only $\langle k\rangle$ other individuals, ignoring variations in node degrees. To accurately predict the dynamics of an epidemic, we need to consider the impact of connectivity patterns, reflected by a network topology, on the epidemic behaviours.

2.2 Complex networks

2.2.1 Network definitions

A network, also called a graph in mathematical terms, is a collection of N nodes (or vertices) joined by M links (or edges). A network is usually visualised as in Fig. 2.4, where circles are referred to as nodes and lines are referred to as links. The size of a network is described by the total number of nodes, N. Two nodes are said to be neighbouring or adjacent if they are connected via a link. The links of a network may be directed or undirected. The directed links represent

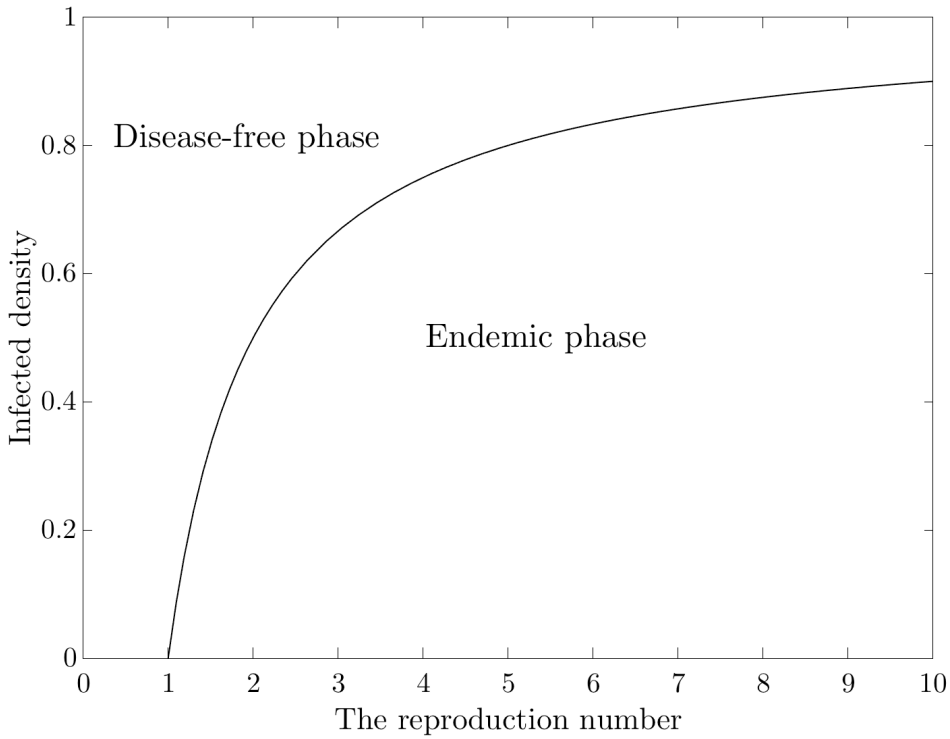

Figure 2.3: Epidemic transition of the classical SIS model. Below the epidemic threshold at $R_0 = 1$, there is no infected density (disease-free phase). Above the epidemic threshold, the infected density attains a nonzero average value at the long time regime (endemic phase).

unidirectional relationships between neighbouring nodes, for example, hyperlinks on the WWW run in one specific direction from one web page to another. On the contrary, the undirected links describe bidirectional relationships, like classmate or co-worker relationship: if you work with Dang, Dang also work with you. A network whose all links are undirected is called an undirected network while a network of directed links is called a directed network.

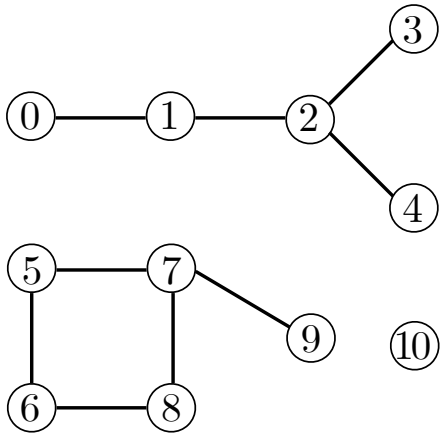

Figure 2.4: A schematic represent of a small network contains eleven nodes and nine links.

A network might contain self-loops, which are links that connect nodes to themselves or multiple links, where there can be more than one link between the same pair of nodes. Link might also have weight which, for instance, express the importance of a connection between pair of nodes. Many interesting networks are weighted, but it is difficult to put down the appropriate numbers [25]. Consequently, these networks often are approximated by an unweighted network.

In the scope of this dissertation, we are interested in a simple network with undirected and unweighted conditions. A simple network means that neither self-loops nor multiple links are allowed in the network.

In the following lists we introduce the basic quantities used to describe and analyse networks.

- **Degrees**: The number of neighbours of a node i or the number of links connected to it is called degree k_i of the node. For example, for the undirected network shown in Fig. 2.4 we have $k_0 = 1, k_1 = 2, k_2 = 3, k_{10} = 0$. In an undirected network the total number of links, M, can be expressed as the sum of the node degrees

$$2M = \sum_{i=1}^{N} k_i. \tag{2.7}$$

The factor 2 comes from the fact that each link has two ends, the total number of ends.

The average degree $\langle k \rangle$ of a node in an undirected network is

$$\langle k \rangle = \frac{1}{N} \sum_{i=1}^{N} k_i = \frac{2M}{N}. \tag{2.8}$$

So in the Fig. 2.4, $\langle k \rangle = 18/11$.

- **Paths**: In network, distance is described by *path length*. A path is a route that runs from node to node along the links of the network. The length of a path represents the number of links traversed along the path. For example, in Fig. 2.4 the path between node 5 to 9 may follow the route $5 \to 6 \to 8 \to 7 \to 9$, hence its length is 4. In general, a path can intersect itself or visit the same node more than once. For example, the path between node 7 and 9 follows $7 \to 5 \to 6 \to 8 \to 7 \to 9$, so node 7 is visited twice.

- **Shortest path**: A shortest path between nodes i and j, denoted by l_{ij}, is a path with the least number of links. If the path intersects itself, then it contains a loop. It can be shortened by avoiding the loop and still connecting between nodes i and j. From the previous example of the path between node 7 and 9, we can remove the loop $7 \to 5 \to 6 \to 8 \to 7$ and the shortest path is $7 \to 9$. It is possible to have multiple shortest paths of equal length between a given pair of nodes (e.g., there are two shortest paths between node 5 and 8: $5 \to 6 \to 8$ and $5 \to 7 \to 8$). Also, it is possible to have no shortest path between two nodes if they are not connected via any route

(e.g., there is no shortest path between node 0 and 5), on the other hand, they are in different components.

- **Components**: A component is a group of connecting nodes in the network– each of which is reachable from the others by some paths through the network. For instance, in Fig. 2.4 there are three components: $\{0, 1, 2, 3, 4\}$, $\{5, 6, 7, 8, 9\}$ and $\{10\}$.

- **Diameter**: The diameter of a network, denoted by $l_{\max}$, is the maximum shortest path between any pairs of nodes in the network. In general the diameter is rarely used as a representation of a network because it only measures the furthest pair, and is unlikely a good indicator of the whole network.

- **Average path length**: The average path length, denoted by $\langle l \rangle$, is the average number of links along the shortest paths for all possible pairs of nodes in the networks. The average path length is more useful as a measure of the behaviour of the network than the diameter.

2.2.2 Erdős-Rényi random network

One of the simplest network models reproducing the real networks is the Erdős-Rényi random network [15–18]. An ER random network contains N nodes and M links where a link between two nodes is placed with probability p. There are two definitions of ER random network:

- $\boldsymbol{G(N, M)}$ **model**: In $G(N, M)$ model, the number of nodes and links are fixed. There are, hence, $\binom{\binom{N}{2}}{M}$ possible graphs that can be formed from the N nodes by chosen M links from all possible pairs, $\binom{N}{2}$ [15–17].

- $\boldsymbol{G(N, p)}$ **model**: The $G(N, p)$ model fixes the probability p that two nodes are connected, but the number of links is not fixed [18].

The two models $G(N, M)$ and $G(N, p)$ are statistically equivalent with $M = p\binom{N}{2}$ [31]. In this dissertation we explore the networks with some constant number of links so we prefer the $G(N, M)$ model than $G(N, p)$.

An ER random network is generated by

1. Create N isolated nodes.
2. Select a pair of nodes randomly. If they are not connected, then connect them with a link and increase the number of pairs. Otherwise, leave them and go to the next step.
3. Repeat step 2 until the total number of pairs is M.

In an ER random network, the degree distribution p_k, which is the probability that a random chosen node has degree k, follows the binomial distribution. However, we are interested in the properties of large networks with a fixed average degree. In some situations, this is more realistic. For example, the typical number of friends a person has does not depend on the total number of people in the world. Moreover, most real networks are sparse meaning that $\langle k \rangle \ll N$. So in this limit with fixed $\langle k \rangle$, the binomial distribution can be approximated by the Poisson distribution

$$p_k = e^{-\langle k \rangle} \frac{\langle k \rangle^k}{k!}. \tag{2.9}$$

The advantage of the Poisson distribution is that it does not depend on the network size, but on the average degree $\langle k \rangle$ only.

One interesting property of an ER random network is the emergence of the largest component. Many real networks typically contain one large component that occupies most of the network (usually more than half of the network size), and numerous number of small components [31]. In ER random network a unique large component or a *giant component* appears when $\langle k \rangle > 1$ [15]. The word giant component has a specific meaning that it is the component whose size grows in proportion to the network size.

ER random network also displays *small world property*, where distance between two randomly chosen nodes in the network is short. The small world effect is found in many real networks. The small world effect predicts that the average path length, $\langle l \rangle$, and the diameter, $l_{\max}$, scales logarithmically with the system size for fixed average degree [6, 32]. So the term *short* means that the value of $\langle l \rangle$ or l_{max} is proportionally to $\ln N$ and grows very slowly with N. The diameter of an ER random network is [6, 31, 32]

$$l_{\max} \approx \frac{\ln N}{\ln\langle k \rangle}. \tag{2.10}$$

The average path length of an ER random network is [33]

$$\langle l \rangle = \frac{\ln N - \gamma}{\ln\langle k \rangle} + \frac{1}{2}, \tag{2.11}$$

where $\gamma \simeq 0.5772$ is the Euler's constant.

Real world networks, however, differ from ER random network. For example, the degree distribution of real networks is scale-free or power law (most nodes have low degree and a few of nodes have high degree) distribution while an ER random network provides the Poisson degree distribution. Despite the disagreement, an ER random network has been widely studied for complex networks. As we can find tremendous papers related to 'random networks/graphs' in Scopus (see http://www.scopus.com/scopus/home.url) and ISI database (see www.webofknowledge.com). The simplicity of an ER random networks makes it possible to compute analytically many properties, particularly with respect to component sizes and average path lengths. Consequently, an ER random network is often used as a baseline model for various applications. Anyway, a random network with non-Poisson degree distribution is developed by Newman [32, 34]. The discussion of this extended model is beyond the scope of this dissertation.

2.2.3 Network dynamics

Complex networks have been generally studied in two aspects of network dynamics. The first aspect is the evolution of particular network structure where the topology

of the network changes as a function of time. There are several possible ways to change topology such as creation and deletion of links, or creation and deletion of nodes [6, 35, 36]. The second aspect is the dynamics on networks where the state of a node (characterised by a discrete variable; for example: active/inactive, spin up/down, susceptible/infected or a scalar variable; for example: density, concentration, flow) changes dynamically in time. In this aspect, the network topology is considered as a static network while the dynamical processes take place, e.g. a disease propagation on a certain network structure.

In most real systems, however, the networks do not have fixed connections for some dynamical processes. Indeed, they evolve in time in response to the dynamics of nodes. Furthermore, the states of nodes change is dependent on the evolution of the topology. In this sense, there is a coupling between the state dynamics and the topological evolution and a feedback loop is formed (Fig. 2.5). The effect of this coupling relies on a dynamic timescale characterised by the time that the node state can change and an evolution timescale which the network topology changes. Faster process is often explored, while slower process is often treated as a constant background influence. If the dynamic timescale is much larger than the evolution timescale, we get an evolving network and can neglect a dynamic state. On the other hand, if the evolution timescale is much larger than the dynamic timescale, then we get a fixed network. However, if the dynamic and evolution are in the same timescale, there is a pure coupling between the state dynamics and the network topology. This network is called an *adaptive network* [10, 14, 37]. An adaptive network establishes many interesting properties such as bifurcations and phase transitions. We will discuss these properties in the following section.

2.3 The SIS model on adaptive networks

When epidemic spreads are modelled in networks, individuals are represented by nodes and the connections between individuals are represented by links of the

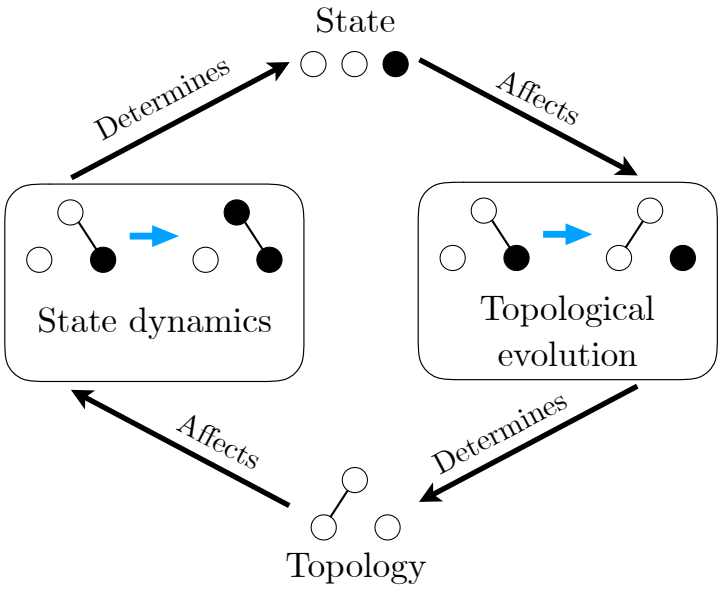

Figure 2.5: Feedback loop shows the coupling between the state dynamics and the topological evolution [14].

network. In SIS adaptive model proposed by Gross et al. [10], there are two main processes: (1) Infection-recovery process which determines the changing of node states, and (2) rewiring process which determines the changing of the network topology. These two processes are coupling that the network structure affects the epidemic spread on the network, while the states of nodes affect the evolution of network topology (see Fig. 2.5).

In this section, we first introduce SIS model on ER random network and some mathematical techniques that are usually used in this approach. After that, the rewiring process is introduced. We note that there are many types of link dynamics to evolve the network topology such as contact-conserving rewiring [10, 38–41], link removal [42], and random link activation and creation [42–44]. In this dissertation, we only follow and develop the adaptive SIS model with contact-conserving rewiring.

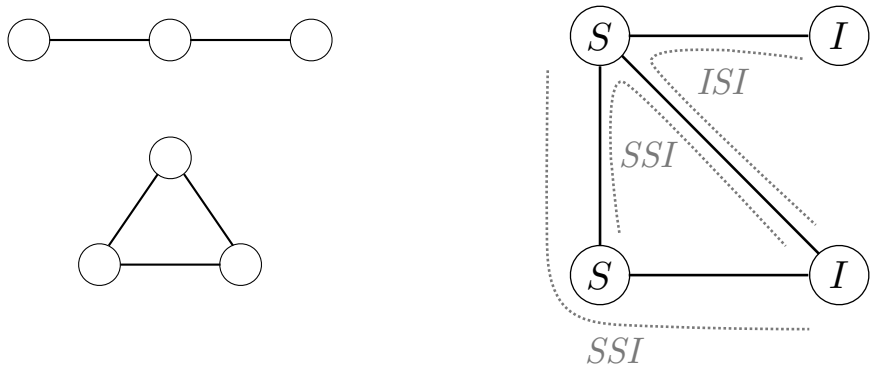

(a) (b)

Figure 2.6: Illustrations of open triplet (figure (a) above) and closed triplet (figure (a) below). The small network (figure (b)) shows that the number of SSI-triplets is two and the number of ISI-triplet is one.

2.3.1 SIS model on networks

In this section we consider quantities related to the dynamics of state and structure. The variables of interest here are typically the average values such as the expected number of nodes ($[A]$), the expected number of links ($[AB]$) and the expected number of triplets ($[ABC]$), with $A, B, C \in \{S, I\}$. A triplet consists of three nodes connected by either two links (open triplet) or three links (closed triplet)–see Fig 2.6. The ordered expression in $[ABC]$ means that a middle node of state B is connected to state A and state C.

Consider random variable $X_i(t)$ that determines the type of node i at time t, for example, $X_i(t) = S$ if node i is susceptible at time t. Then the expected values can be defined as

$$\begin{aligned}
[A](t) &= \sum_{i=1}^{N} \text{Prob}(X_i(t) = A), \\
[AB](t) &= \sum_{i=1}^{N}\sum_{j=1}^{N} a_{i,j}\text{Prob}(X_i(t) = A, X_j(t) = B), \\
[ABC](t) &= \sum_{i=1}^{N}\sum_{j=1}^{N}\sum_{k=1}^{N} a_{ij}a_{jk}\text{Prob}(X_i(t) = A, X_j(t) = B, X_k(t) = C),
\end{aligned} \tag{2.12}$$

where $A, B, C \in S, I$ and a_{ij} is one if node i connects to node j; otherwise it is

zero.

These expected values of nodes and links obey conservation relations. The conservation for the node is based on the fact that $\text{Prob}(X_i(t) = S)+\text{Prob}(X_i(t) = I) = 1$ for $i = 1, \ldots, N$. This implies that

$$[S](t) + [I](t) = N, \tag{2.13}$$

for any time t. Similarly, the conservation relation of the links following four states SS, SI, IS and II is

$$[SS](t) + [SI](t) + [IS](t) + [II](t) = \sum_{i=1}^{N}\sum_{j=1}^{N}(1)a_{ij} = \langle k\rangle N,$$

where $\langle k\rangle$ is the average degree defined in Section 2.2.1. Since SI-links and IS-links are symmetrical, we can count $[IS]$ as $[SI]$. Thus we reduce the above equation to

$$[SS](t) + [SI](t) + [II](t) = \langle k\rangle N. \tag{2.14}$$

From now on, we drop the explicit t-dependence of $[A](t)$, $[AB](t)$ and $[ABC](t)$ for convenience.

In the classical SIS model, the fully-mixed assumption approximates the infection term in Eq. 2.1 to $b\langle k\rangle[S][I]/N$. With contact base, instead, this can be written exactly as $b[SI]$ where $[SI]$ is the expected number of links between susceptible and infected nodes. So we obtain the dynamic of nodes with the pairwise term:

$$\begin{aligned}\frac{d[S]}{dt} &= r[I] - b[SI],\\ \frac{d[I]}{dt} &= b[SI] - r[I].\end{aligned} \tag{2.15}$$

Eqs. 2.15 show that the dynamic of nodes depends on the number of SI-links. Therefore this set of equations is not closed. To close the equations, one employs the *mean-field approximation*, in which the number of SI-links is approximated by $[SI] \approx \langle k\rangle[S][I]/N$ [37]. Eqs. 2.15 can be closed as

$$\begin{aligned}\frac{d[S]}{dt} &= r[I] - b\frac{\langle k\rangle}{N}[S][I],\\ \frac{d[I]}{dt} &= b\frac{\langle k\rangle}{N}[S][I] - r[I].\end{aligned} \tag{2.16}$$

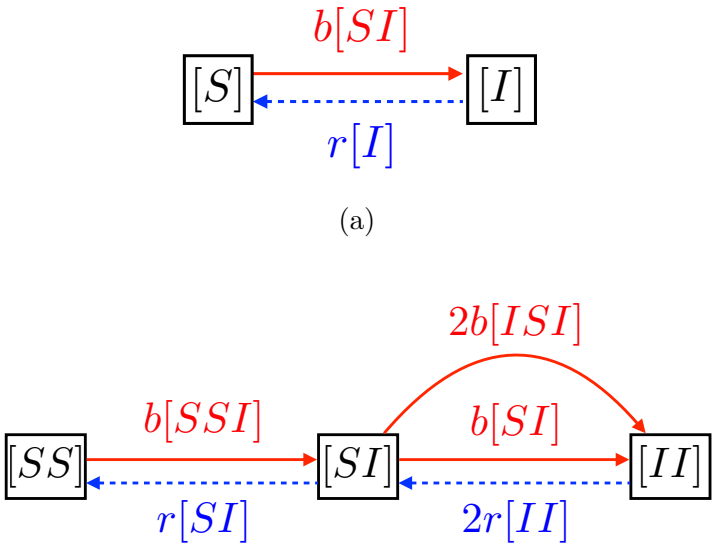

(a)

(b)

Figure 2.7: Flow diagrams show the flux between compartments of nodes (figure (a)) and compartments of links (figure (b)). Solid lines denote the infection process coming from an infected node with the rate depending on a link or a triplet. Dashed lines denote the recovery process.

In this approximation, however, all structural properties of the network are neglected, except for the average degree $\langle k \rangle$. This means that the dynamics of links cannot be taken into account in this approximation.

To capture the effects of the topological changes, we need to treat compartments of links as dynamical variables. To write down the rate equations for the dynamics of links, we construct a flow diagram directly derived from the infection-recovery process for SIS model (see Fig. 2.7). To close Eqs. 2.15, we need additional dynamical equations for links. From the flow diagram in Fig. 2.7b, SS-links are created by recovery at rate $r[SI]$ and destroyed by an infection event due to infected neighbours outside the SS-links at rate $b[SSI]$. So we obtain the rate equation for $[SS]$:

$$\frac{d[SS]}{dt} = r[SI] - b[SSI]. \tag{2.17}$$

For the II-links, a recovery event can destroy II-links if a recovered node is in such a link. Since one II-link consists of two infected nodes, the total rate

at which II-links are destroyed is $2r[II]$. II-links can be created by two infection events. The first one comes from the infection spreading across a SI-link converting the link into II-link at rate $b[SI]$. The second event occurs due to the infection of infected nodes in ISI-triplets which creates two II-links so this event occurs at rate of $2b[ISI]$. Thus the rate equation for $[II]$ is

$$\frac{d[II]}{dt} = b(2[ISI] + [SI]) - 2r[II]. \tag{2.18}$$

From the conservation relation of links (Eq. 2.14), the rate equation of $[SI]$ is

$$\frac{d[SI]}{dt} = 2r[II] + b([SSI] - 2[ISI]) - (b + r)[SI]. \tag{2.19}$$

Again, this system of Eqs. 2.15–2.19 does not yield a closed form and involves the triplets of $[SSI]$ and $[ISI]$. In order to close the system, *pair approximation* is used here to approximate the triplets [37, 45, 46]:

$$[ABC] \approx \frac{\langle q \rangle}{\langle k \rangle} \frac{[AB][BC]}{[B]} \frac{\mu_{AB}\mu_{BC}}{\mu_{AC}}, \tag{2.20}$$

where $\mu_{AB} = 1 + \delta_{AB}$ denotes the double-counting of symmetric triplets and $\langle q \rangle$ is the *mean excess degree* which is the average number of additional links connected to B-node found by following a random link. According to Rand [45], the pair approximation is considered for two types of distributions: Poisson distribution and multinomial distribution. In this work, we consider ER random network with large network size and fixed mean degree. Therefore, the degree distribution is Poisson distribution (Sec. 2.2.2). For simplicity, the adaptive network is approximated to be random network, to which a random-graph-like approximation is applied [37]. With this assumption, $\langle q \rangle \approx \langle k \rangle$. Consequensely, we can approximate the expected number of triplets as

$$[SSI] = \frac{2[SS][SI]}{[S]}, \qquad [ISI] = \frac{[SI]^2}{2[S]}. \tag{2.21}$$

The approximation is under assumption that links are distributed homogeneously in the network [46]. Substituting these relations into Eqs. 2.17, 2.18 and 2.19, we

obtain a closed system of differential equations

$$\begin{aligned}
\frac{d[S]}{dt} &= r[I] - b[SI], \\
\frac{d[I]}{dt} &= b[SI] - r[I], \\
\frac{d[SS]}{dt} &= r[SI] - 2b\frac{[SS][SI]}{[S]}, \\
\frac{d[II]}{dt} &= b[SI]\left(1 + \frac{[SI]}{[S]}\right) - 2r[II], \\
\frac{d[SI]}{dt} &= 2r[II] + b[SI]\left(\frac{2[SS] - [SI]}{[S]}\right) - (b + r)[SI].
\end{aligned} \tag{2.22}$$

The pair approximation only requires basic information of link and node distributions that are available in most network model. This approximation is more realistic to study local behaviour of network such as infection process which cannot be accurately determined by using fully mixed approximation. Furthermore, if link distribution is properly sampled, this approximation can be used to represent of entire network. However, the pair approximation neglects higher-order network structure such as stars and triangles. This makes less accurate to model highly clustering network where correlation is very localised [8].

2.3.2 Describing the SIS adaptive network model

In this section, we briefly review the work given by Gross et al. [10], where epidemic spread is studied on the adaptive SIS network model. As an adaptation strategy to avoid infection, susceptible nodes are allowed to remove their links with infected neighbours with rewiring rate w, and the susceptible node immediately finds a randomly chosen susceptible node to reconnect once the original link is cut off.

To analyse the adaptive network for SIS model, the system of Eqs 2.22 is modified. We can reduce five dynamical variables down to three by using conservation relations (Eqs. 2.13 and 2.14). The rate equations with rewiring mechanism

are

$$\begin{aligned}
\frac{d[I]}{dt} &= b[SI] - r[I], \\
\frac{d[SS]}{dt} &= r[SI] - 2b\frac{[SS][SI]}{1-[I]} + \underbrace{w[SI]}_{\text{gain due to rewiring}}, \\
\frac{d[SI]}{dt} &= 2r(1-[SS]-[SI]) + b[SI]\left(\frac{2[SS]-[SI]}{1-[I]}\right) - (b+r)[SI] - \underbrace{w[SI]}_{\text{loss due to rewiring}}.
\end{aligned} \tag{2.23}$$

The term $w[SI]$ is added to the rate equations of $[SS]$ and $[SI]$ because each rewiring event creates new SS-link and destroys SI-link. Even if the system contains three dynamical parameters, b, r and w, it can be reduced to two independent dimensionless ratios namely b/r and w/r. Physically speaking, this is equivalent to rescaling time by the infection period r^{-1}. Thus we obtain the rescaling form of Eqs. 2.23:

$$\begin{aligned}
\frac{d[I]}{dt} &= b[SI] - [I], \\
\frac{d[SS]}{dt} &= [SI] - 2b\frac{[SS][SI]}{1-[I]} + w[SI], \\
\frac{d[SI]}{dt} &= 2(1-[SS]-[SI]) + b[SI]\left(\frac{2[SS]-[SI]}{1-[I]}\right) - (b+w+1)[SI],
\end{aligned} \tag{2.24}$$

where b and w are rescaled parameters.

It is convenience to consider the density of node and links. Node density can be defined as

$$[s] \equiv \frac{[S]}{N} \quad \text{and} \quad [i] \equiv \frac{[I]}{N}, \tag{2.25}$$

and link density as

$$[ss] \equiv \frac{[SS]}{M}, \quad [ii] \equiv \frac{[II]}{M} \quad \text{and} \quad [si] \equiv \frac{[SI]}{M}. \tag{2.26}$$

Using the definition of average degree $\langle k \rangle = 2M/N$, we obtain a closed three-

dimensional system of rate equations:

$$\begin{aligned}
\frac{d[i]}{dt} &= \frac{b\langle k\rangle}{2}[si] - [i], \\
\frac{d[ss]}{dt} &= (w+1)[si] - b\langle k\rangle \frac{[ss][si]}{1-[i]}, \\
\frac{d[si]}{dt} &= 2(1-[ss]-[si]) + \frac{b\langle k\rangle}{2}[si]\left(\frac{2[ss]-[si]}{1-[i]}\right) - (b+w+1)[si].
\end{aligned} \tag{2.27}$$

To prevent and control infection, we can use phase diagram as a guideline. So in this work, we study phase diagram of epidemics which shows all possible outcomes of a network. The phase diagram is usually compute from the steady state conditions. At the steady state we observe the epidemic transition between the disease-free state and the endemic state. We start from the Jacobian matrix at an arbitrary point

$$\mathbf{J} = \begin{pmatrix}
-1 & 0 & \frac{b\langle k\rangle}{2} \\
-b\langle k\rangle \frac{[ss][si]}{(1-[i])^2} & -b\langle k\rangle \frac{[si]}{1-[i]} & w+1-b\langle k\rangle \frac{[ss]}{1-[i]} \\
\frac{b\langle k\rangle}{2}\frac{2[ss][si]-[si]^2}{(1-[i])^2} & b\langle k\rangle \frac{[si]}{1-[i]} - 2 & b\langle k\rangle \frac{[ss]-[si]}{1-[i]} - b - w - 3
\end{pmatrix}$$

For the disease-free state, $([i],[ss],[si]) = (0,1,0)$, so $\mathbf{J}$ reduces to

$$\mathbf{J} = \begin{pmatrix}
-1 & 0 & \frac{b\langle k\rangle}{2} \\
0 & 0 & w+1-b\langle k\rangle \\
0 & -2 & b\langle k\rangle - b - w - 3
\end{pmatrix}.$$

To find the eigenvalues λ of the Jacobian matrix, we solve

$$\begin{aligned}
\det(\mathbf{J} - \lambda \mathbf{I}) &= 0 \\
(\lambda+1)(\lambda^2 + \lambda(2+b-\alpha) - 2\alpha) &= 0,
\end{aligned}$$

where $\alpha = b\langle k\rangle - w - 1$. One eigenvalue is $\lambda_1 = -1$, and other two eigenvalues are

$$\lambda_{\pm} = \frac{(\alpha - b - 2) \pm \sqrt{(\alpha-b-2)^2 + 8\alpha}}{2}. \tag{2.28}$$

If the real part of all eigenvalues are negative, then the steady state is stable. If at least one eigenvalue has a positive real part, then the steady state is unstable. Consider Eq. 2.28 if $\alpha < 0$, then $\mathrm{Re}(\lambda_+) < 0$ and $\mathrm{Re}(\lambda_-) < 0$. On the other hand, if $\alpha > 0$, then $\mathrm{Re}(\lambda_+) > 0$ and $\mathrm{Re}(\lambda_-) < 0$. Therefore the disease-free state is stable if $\alpha < 0$ or $b\langle k\rangle - w - 1 < 0$ and the state loses stability if $\alpha > 0$. This implies the critical value of infection rate

$$b_c = \frac{w+1}{\langle k\rangle}, \tag{2.29}$$

which is called the *epidemic threshold* [47]. Note that this corresponds to $b_c = r/\langle k\rangle$ for $w = 0$.

At the steady state of Eqs. 2.27 for $[i] \neq 0$, we can obtain the link variables, $[ss]$ and $[si]$, as a function of $[i]$:

$$\begin{aligned} [si] &= \frac{2}{b\langle k\rangle}[i], \\ [ss] &= \frac{w+1}{b\langle k\rangle}(1-[i]). \end{aligned} \tag{2.30}$$

Substituting Eqs. 2.30 into $\dfrac{d[si]}{dt} = 0$, then we have the quadratic equation of $[i]$ as

$$(b-w)[i]^2 - (b\langle k\rangle + b - 2w)[i] + (b\langle k\rangle - w - 1) = 0 \tag{2.31}$$

whose solutions are

$$[i] = \frac{b\langle k\rangle + b - 2w \pm \sqrt{\,b^2(\langle k\rangle - 1)^2 + 4(b-w)}}{2(b-w)}. \tag{2.32}$$

For a static epidemic network $w = 0$, the solutions in Eq. 2.32 become

$$\begin{aligned} [i]_1 &= \frac{b(\langle k\rangle + 1) + \sqrt{\,b^2(\langle k\rangle - 1)^2 + 4b}}{2b}, \\ [i]_2 &= \frac{b(\langle k\rangle + 1) - \sqrt{\,b^2(\langle k\rangle - 1)^2 + 4b}}{2b}. \end{aligned} \tag{2.33}$$

The solution $[i]_1$ is always larger than one, so it is unphysical. Consider the remaining solution $[i]_2$, if $b > 1/\langle k\rangle$, then $0 < [i]_2 < 1$; otherwise $[i]_2 < 0$. Combine

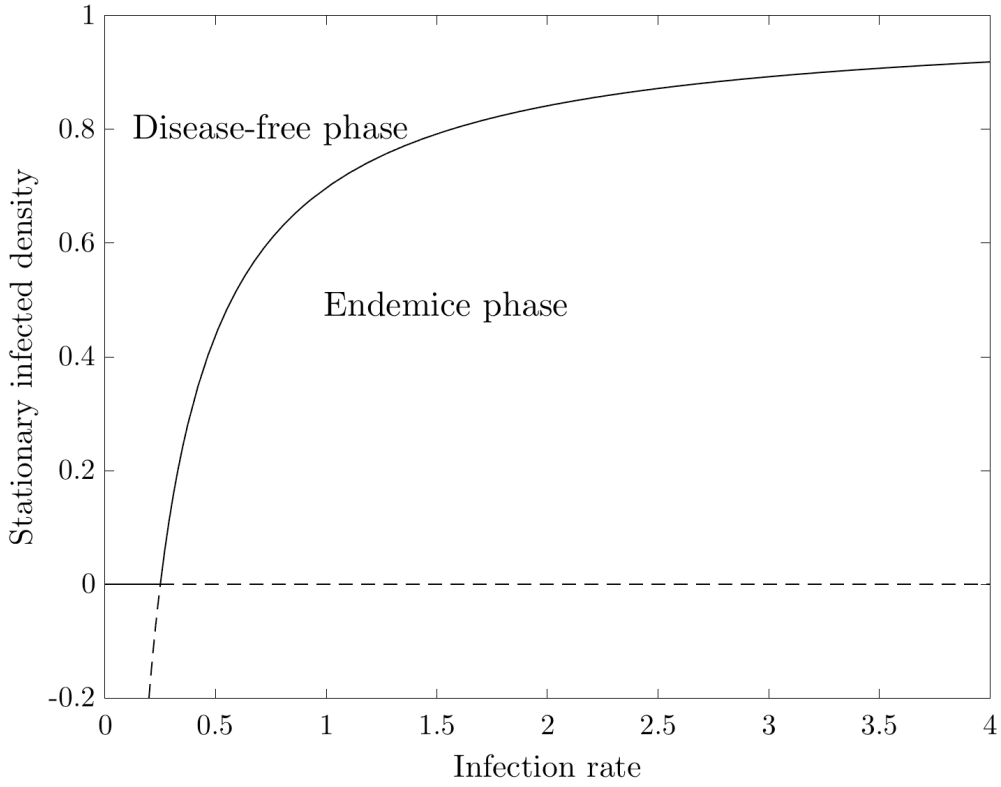

Figure 2.8: Bifurcation diagram of the SIS model on ER random network shows the stationary infected density ($[i]_\infty$) as a function of the infection rate. Solid lines show stable solutions whereas dashed lines show unstable solutions. In disease-free phase, $[i]_\infty = 0$ is stable below the critical infection rate and in endemic phase, $[i]_\infty > 0$ becomes stable. The unstable stationary state $[i]_\infty < 0$ is a non-physical solution. This plot uses $\langle k \rangle = 4$.

this solution to the trivial solution, $[i] = 0$, in the disease-free state, we obtain the epidemic transition as shown in Fig. 2.8. At small infection rate below the epidemic threshold, there is no infected node left in the network indicating that the network is in a disease-free phase. For large infection rate above the epidemic threshold, there is the persistence of infected nodes indicating an endemic phase. These results yield the epidemic threshold corresponding to the classical SIS model (Fig. 2.3), with reproduction number $R_0 = b_c\langle k \rangle / r = 1$.

For the adaptive network case ($w \neq 0$), at the epidemic threshold $b_c =$

$(w+1)/\langle k\rangle$, there are two solutions

$$\begin{aligned} [i]_1 &= 0, \\ [i]_2 &= \frac{b\langle k\rangle + b - 2w}{b-w}. \end{aligned} \tag{2.34}$$

Then two endemic steady states exist for some set of parameters $\langle k\rangle, b$ and w. Gross et al. [10] observed that there is another threshold corresponding to a saddle-node bifurcation. Kiss et al. [47] claimed that this threshold is on the parabola $w = \frac{b^2(\langle k\rangle - 1)^2 + 4b}{4}$. Combine these two thresholds, we obtain bifurcation diagram in Fig. 2.9. With rewiring mechanism, therefore, a region of stable solutions of both endemic and disease-free states exists.

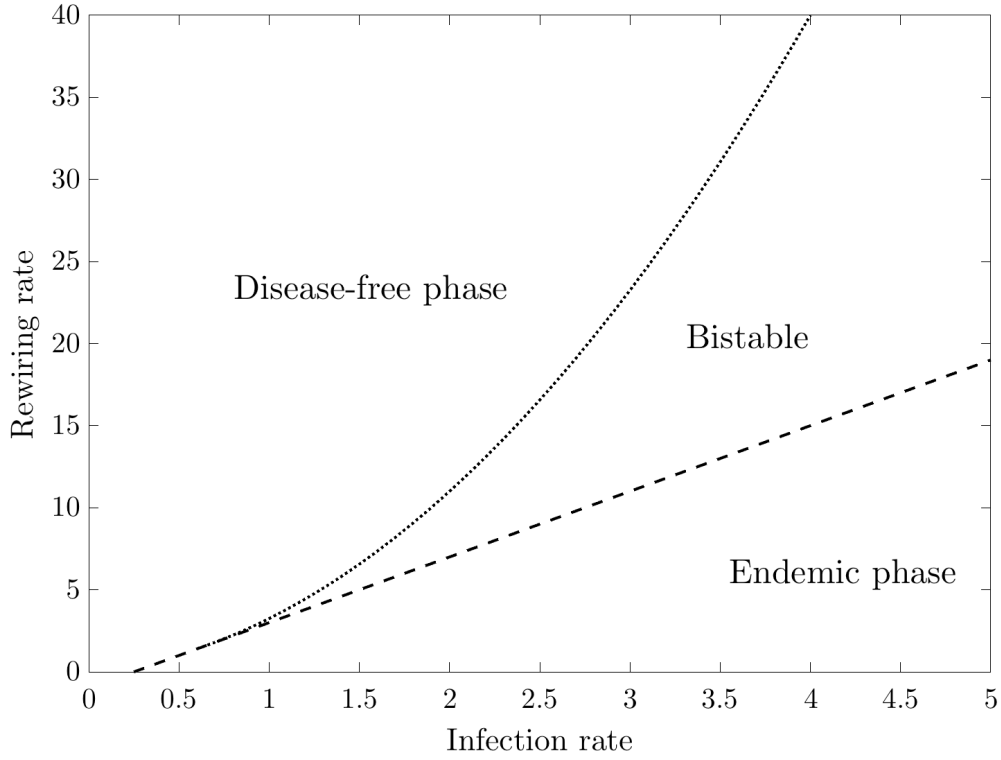

Figure 2.9: Two-parameter bifurcation diagram shows the dependence on the infection rate and the rewiring rate for $\langle k \rangle = 4$. The dashed and dotted lines are transition lines corresponding to transcritical and saddle-node bifurcation, respectively. Below the dashed line, there is only endemic state while above the dotted line there is only disease-free state. Between these two transition lines, networks can be either endemic or disease-free state.

CHAPTER III

Analysis and modelling method

In the past two decades, epidemic models on adaptive networks have gotten more attention [10, 11, 38, 39, 42–44, 48]. Many strategies to model the real-world behaviours are proposed such as contact-conserving rewiring [10, 38, 39], link removal [42], and random link activation and creation [42–44]. In these models, a decision to change contact is based on information known globally, i.e., everyone knows the health status of all others in the network. This concept, however, is not practical in real life for large network. For example, a college student may not know health statuses of every one of her classmates. Even if it is possible for a node to know the status of each other such as computers in a network, storing this information consumes significant time and memory space. Thus we propose a more practical method where decision is based on local information. The word "local" means that there is a limited distance where information can be transmitted. In a network, distance is defined through a path (section 2.2.1) so we define the local area as the neighbourhood of a node. In this chapter we discuss our proposed method called local rewiring method and how to simulate the adaptive epidemic network with local rewiring. Equations describing the evolution of this network are also described.

3.1 An adaptive SIS model with local rewiring

According to section 2.3.2, a susceptible node who makes contact with an infected node may decide to break this SI-link and create a new link with another

non-contact susceptible node. This decision assumes that the node that wants to rewire away must possess information about every node in the network so it can make the decision. We call the original rewiring method [10] *global rewiring* method. In order to make rewiring more realistic, we modify the existing rewiring method based on the neighbouring information such that the rewiring takes this information into account when identifying candidate nodes for rewiring. We called our proposed method *local rewiring*.

In the local rewiring mechanism, determining who are neighbours of a node is required. We introduce a new quantity called *neighbouring distance* d which is the maximum distance where information about health statuses of neighbours are known. The neighbouring distance is defined through the shortest path from a given node. For example, in Fig. 3.1, with $d = 3$, neighbours of the black node are the nodes in the dashed circle where the first-order neighbourhood of the black node is the set of the nearest neighbours of the node, the second-order neighbourhood is the set of the second-nearest neighbours, etc. In the local rewiring, a node is allowed to rewire within their neighbourhood. In the Fig. 3.1 with $d = 3$, the black node knows the health status of every nodes in the dashed circle, then the node is able to rewire to any susceptible nodes in the regions B and C. Note that we consider a simple network where self-loops and multiple links are not allowed so the node cannot rewire to itself or to its nearest neighbours to avoid double links. To simplify the model, we set the neighbouring distance to be constant for every node in the network. Fig. 3.2 shows the differences between global and local rewiring.

3.2 Analytic approach

The node and link densities are defined as

$$\begin{aligned} [s_g] = \frac{[S_g]}{N_g} \quad \text{and} \quad [i_g] = \frac{[I_g]}{N_g}, \\ [ss_g] = \frac{[SS_g]}{M_g}, \quad [ii_g] = \frac{[II_g]}{M_g} \quad \text{and} \quad [si_g] = \frac{[SI_g]}{M_g}. \end{aligned} \tag{3.1}$$

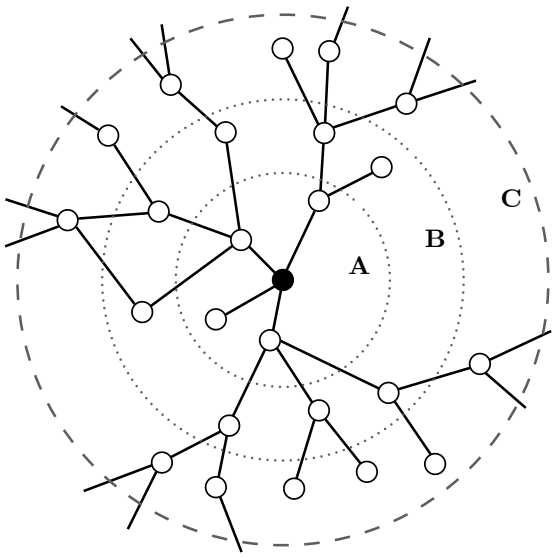

Figure 3.1: A schematic represents neighbours of a node with a neighbouring distance $d = 3$. Consider the black node, the set of the white nodes inside the region A is in first-order neighbourhood, the set of the white nodes inside the region B is in the second-order neighbourhood and the set of the white nodes inside the region C is in the third-order neighbourhood. With $d = 3$, every node in dashed circle is a neighbour of the black node.

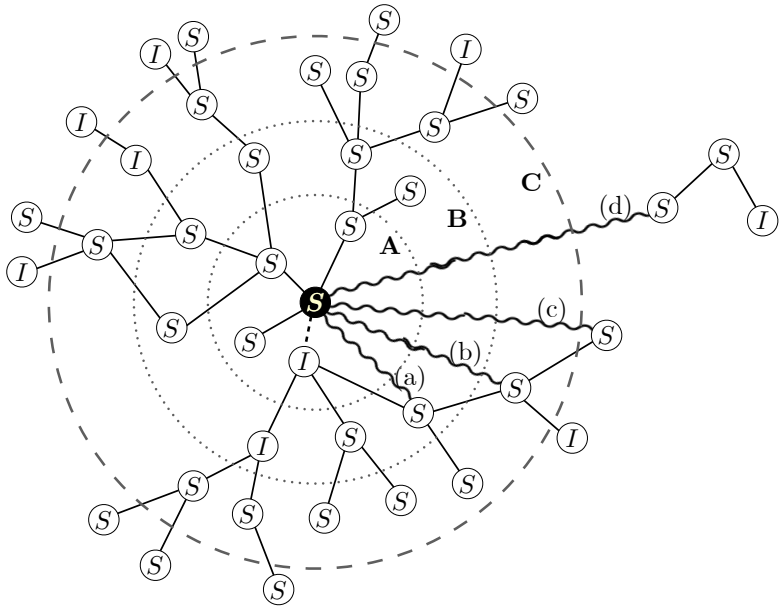

Figure 3.2: A schematic represents some possible rewiring events for the global rewiring and the local rewiring with the neighbouring distance $d = 3$. In the global rewiring method, the black node who is susceptible breaks the SI-link (dashed line) and may create new SS-link (wavy lines) with any S-node in (a) the second-order neighbourhood, (b) the third-order neighbourhood, (c) the fourth-order neighbourhood or (d) another component. In the local rewiring method, the node is allowed only to rewire within the neighbouring distance ($d = 3$) which is in the case of (a) or (b). Notice that neighbours of the node are observed before the taking place of rewiring event. After the rewiring, neighbours of the node will be updated. Figure reprinted from [49].

The subscript g signifies that the quantities of interest are those of the giant component. For other components such as small components, their evolution tends to typically of size one due to the local rewiring (we will explain more in the next chapter). Eventually, all nodes in the small components are susceptible and there is no dynamics. Therefore we are interested in the giant component rather than the whole network. With these definitions, we obtain the conservation of nodes and links, the same as in Eqs. 2.13 and 2.14

$$[s_g] + [i_g] = 1 \quad \text{and} \quad [ss_g] + [ii_g] + [si_g] = 1. \tag{3.2}$$

A node in ER random network has on average:
$\langle k \rangle$ at distance one,
$\langle k \rangle^2$ at distance two,
$\langle k \rangle^3$ at distance three,
...
$\langle k \rangle^d$ at distance d.
Then the average number of neighbours of a node at distance d is

$$N_d \approx \langle k \rangle + \langle k \rangle^2 + \ldots + \langle k \rangle^d = \langle k \rangle \frac{\langle k \rangle^d - 1}{\langle k \rangle - 1}. \tag{3.3}$$

Assume that $\langle k \rangle \gg 1$ the equation becomes

$$N_d \approx \langle k \rangle^d. \tag{3.4}$$

For example, if $\langle k \rangle = 10$ and $d = 4$, then $N_d \approx 10^4 = 10,000$. In this work, we consider the network size up to 10,000 so the value of N_d may exceed the network size such that N_d is set to the giant component size N_g.

$$N_d = N_g. \tag{3.5}$$

Among the N_g neighbours, there are roughly $[S_g]$ susceptible nodes to which a susceptible node can rewire. Thus the probability that the susceptible node in the giant component has susceptible neighbours is $[S_g]/N_g$. In the local rewiring with

rewiring rate w_d, therefore, the rewiring event occurs at the rate of $w_d[S_g]/N_g = w_d[s_g]$. Eqs. 2.27 are modified to

$$\begin{aligned}
\frac{d[i_g]}{dt} &= \frac{bk_g}{2}[si_g] - [i_g], \\
\frac{d[ss_g]}{dt} &= \big(\underbrace{w_d(1-[i_g])}_{\text{local rewiring}} + 1\big)[si_g] - bk_g\frac{[ss_g][si_g]}{1-[i_g]}, \\
\frac{d[si_g]}{dt} &= 2(1-[ss_g]-[si_g]) + \frac{bk_g}{2}[si_g]\left(\frac{2[ss_g]-[si_g]}{1-[i_g]}\right) - \big(b + \underbrace{w_d(1-[i_g])}_{\text{local rewiring}} + 1\big)[si_g],
\end{aligned} \tag{3.6}$$

where k_g is the mean degree of a node in the giant component.

3.3 Kinetic Monte Carlo simulation

To study the stochastic process of epidemic spreads on a network, we perform a stochastic node-based simulation by keeping track of all possible events in the network and the rates at which these events happen. We consider the node-based selection where an S node is chosen randomly and, if the S-node connects to an I node, it is rewired to a randomly chosen available susceptible node. To perform this simulation, we model the adaptive SIS network with continuous-time Monte Carlo method with event driven algorithms, also called kinetic Monte Carlo (kMC) simulation [21–24].

Consider adaptive SIS dynamics taking place on a network of N nodes and M links. At any time t each node i has a corresponding state X_i^t, which is either susceptible ($X_i^t = S$) or infected ($X_i^t = I$), and each link between node i and j has a corresponding state Y_{ij}^t, which can be one of: SS-link ($Y_{ij}^t = SS$), II-link ($Y_{ij}^t = II$) or SI-link ($Y_{ij}^t = SI$). There are three processes of an adaptive SIS network including:

1. Recovery process which acts on I-nodes. This event occurs at recovery rate of r for each I-node.

2. Infection process which acts along SI-links. The infection rate per link is b, therefore the total infection rate of a given S-node who has k_i infected neighbours is $k_i b$.

3. Local rewiring process which acts along SI-links. A given S-node who has infected neighbour(s) may rewire to non-adjacent node who is susceptible and one of the S-node's neighbours N_d. For the local rewiring with neighbouring distance d, the rewiring occurs at rate w_d.

These processes can be defined in terms of probabilities as [50]

$$\begin{aligned} r &= \lim_{\Delta t \to 0} \frac{P(X_i^{t+\Delta t} = S | X_i^t = I)}{\Delta t}, \\ b &= \lim_{\Delta t \to 0} \frac{a_{ij}^t P(X_i^{t+\Delta t} = I, X_j^{t+\Delta t} = I | X_i^t = S, X_j^t = I)}{\Delta t}, \\ w_d &= \lim_{\Delta t \to 0} \frac{a_{ij}^t (1 - a_{il,l\in N_d}^t)(1 - a_{ij}^{t+\Delta t}) a_{il,l\in N_d}^{t+\Delta t} P(Y_{il,l\in N_d}^{t+\Delta t} = SS | Y_{ij}^t = SI)}{\Delta t}, \end{aligned} \tag{3.7}$$

where $a_{ij}^t = 1$ when nodes i and j are adjacency at time t, otherwise a_{ij}^t is zero. For the local rewiring process with neighbouring distance d, the rewire-to S-node must be in the set of N_d.

The fraction terms on the right hand sides of Eqs. 3.7 are the transition probabilities per unit time. Taking the limit as $\Delta t \to 0$ leads to the concept of transition rates. We define the transition rate W_i as

$$W_i = \begin{cases} ib & \text{for } i = 0, 1, ..., N-1 \\ r & \text{for } i = N, \\ w_d & \text{for } i = N+1. \end{cases} \tag{3.8}$$

For $i = 0, ..., N-1$ the transition rates W_i are the total infection rate for each S-node who has i infected neighbours. For $i = N$ and $N+1$, W_i are the transition rate of recovery and rewiring, respectively. After weighing the transition rate W_i

with its number of events, we obtain the rate

$$R_i = \begin{cases} ib[S]_i & \text{for } i = 0, 1, ..., N-1 \\ r[I] & \text{for } i = N, \\ w_d[SI] & \text{for } i = N+1, \end{cases} \tag{3.9}$$

where $[S]_i$ is the number of S-nodes with i infected neighbours. The sum of the rates is denoted by

$$R = \sum_{i=0}^{N+1} R_i. \tag{3.10}$$

In continuous-time dynamics, these processes cannot happen simultaneously [51]. When a node is infected, we are able to calculate with a well-prescribed probability when it will recover. For a susceptible node who has infected neighbour(s), we calculate when its neighbour(s) will transmit a disease to and when it will rewire to another susceptible. We construct the probability distribution of these events according to as follows [51, 52]:

(a) The probability that no event occurs in the time interval $(t_0 = 0, t)$ [21–23] is

$$P(t) = \exp(-Rt). \tag{3.11}$$

The probability that any event occurs in the interval $(t, t+dt)$ is $p(t)dt$. Thus the total probability that any event occurs in the time interval $(t_0 = 0, t)$ is

$$\int_{t_0=0}^{t} p(t)dt = 1 - P(t). \tag{3.12}$$

This represents a distribution with mean waiting time τ that the network remains in its current state before changing to the next state where

$$\tau = \int_{t_0=0}^{\infty} tp(t)dt = \frac{1}{R}. \tag{3.13}$$

(b) The probability that an event i will be selected is $R_i / \sum_{j=1}^{N+1} R_j$.

These are the basis of the kMC simulation [51] which is an event-driven algorithm. Time interval is not fixed but rather corresponds to the time between

consecutive changes in the network. At each step, time advances by an amount τ and node i changes its state or link, where τ and i are random numbers drawn (see Fig. 3.3). Once the system has been initialised, the algorithm then consists of the following steps that are iterated until either the chosen final time is reached, or the network reaches the disease-free state where there is no evolution anymore:

1. At each time step, compute transition rate W_i and weigh it with the number of events for each rate. The total rate $R = \sum_{i=0}^{N+1} R_i$ is calculated. Then the cumulative rates $C_l \equiv \sum_{i=1}^{l} R_i$ is drawn (see Fig. 3.4).

2. Randomly select a process with a probability given by item (b). Thus an event l is selected such that $C_l \geq \rho_1 R > C_{l-1}$, where ρ_1 is a random number uniformly distributed in the interval $(0, 1)$.

3. Event l is executed and time t is updated according to item (a). Waiting time τ is drawn from a Poisson distribution [21, 22, 51] as

$$\tau = -\frac{\ln(\rho_2)}{W}, \tag{3.14}$$

where ρ_2 is a random number distributed uniformly in the interval $(0, 1)$. Therefore the physical time advanced in a single step is $t \to t + \tau$.

Our kMC simulation is illustrated as a flowchart in Fig 3.5.

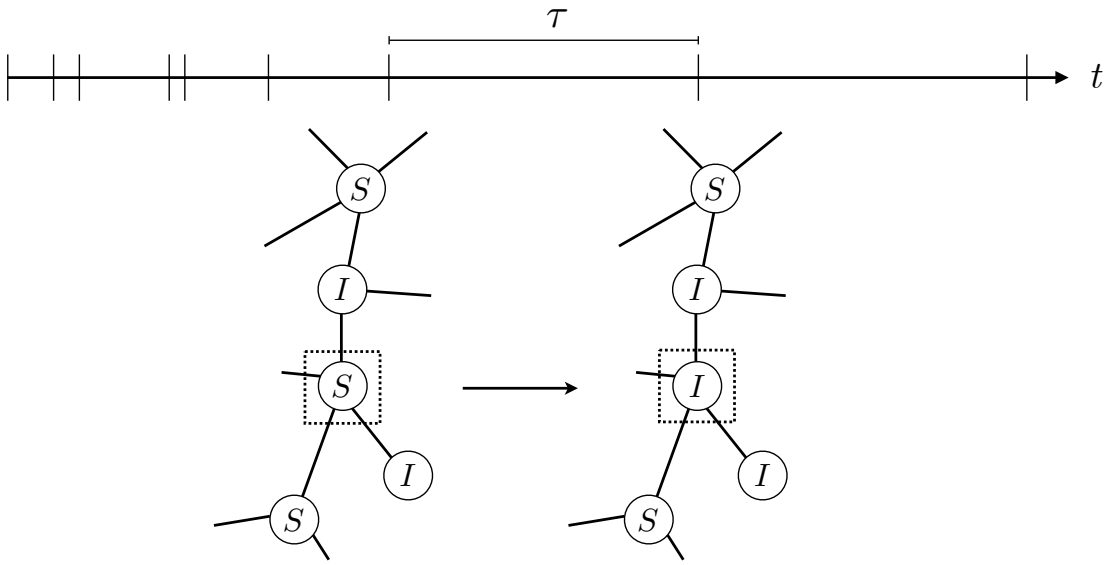

Figure 3.3: A Schematic of the kMC algorithm. Vertical ticks on the t axis indicate the moments when the simulation advances. The interval time τ is given by item (a). The square around a node shows that the node has been chosen for updating. This node is chosen according to item (b).

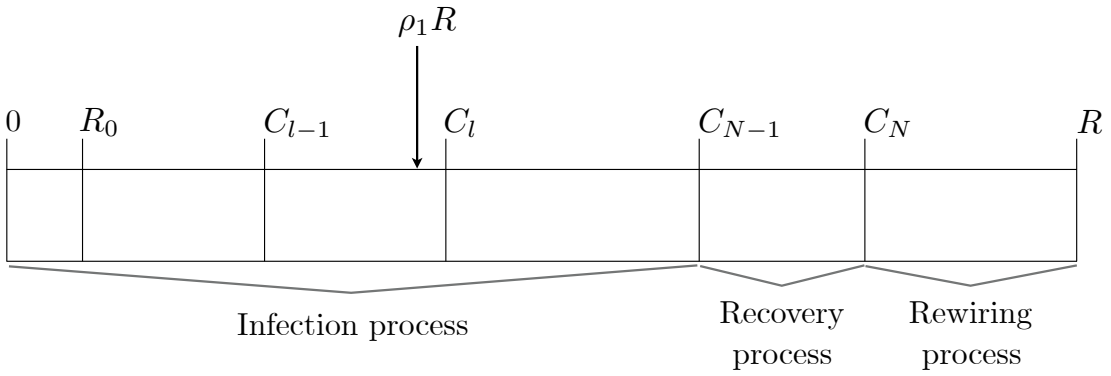

Figure 3.4: A schematic representation of the lth event selection.

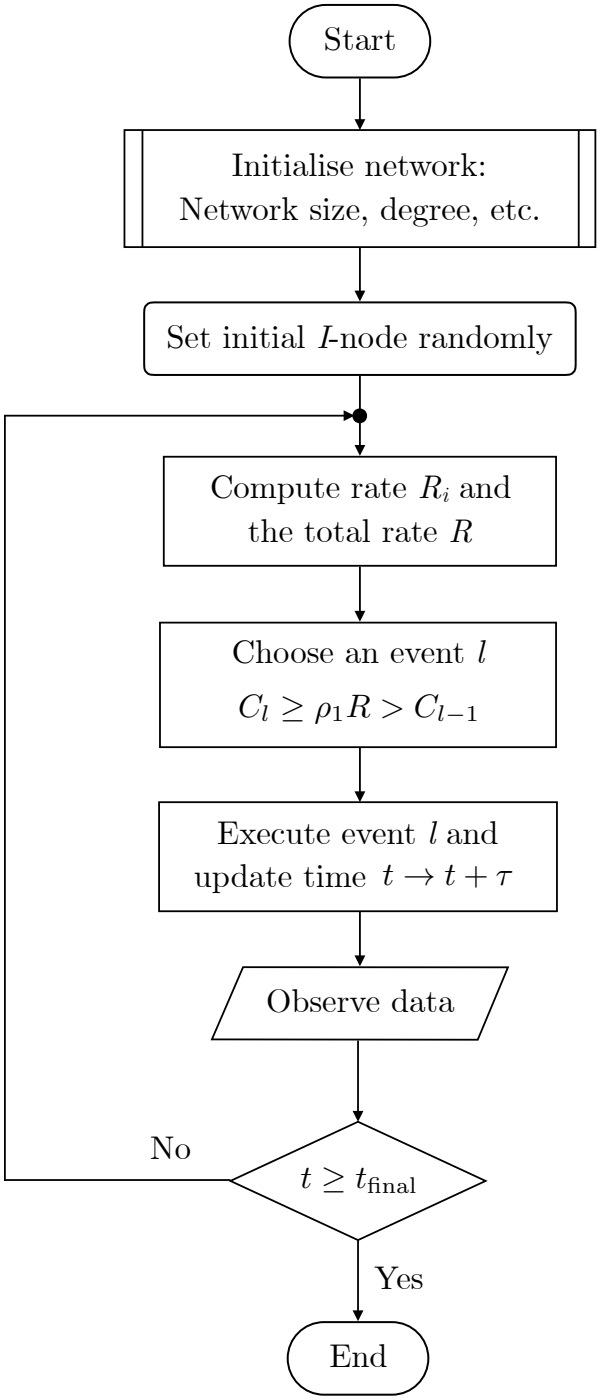

Figure 3.5: A flowchart of kMC simulation.

CHAPTER IV

Results and Discussions

In this chapter, we discuss our numerical results of epidemic spreading on adaptive networks at different neighbouring distances and network sizes. The main goal is to investigate the effects due to local rewiring and global rewiring processes. In this work, we simulate the adaptive SIS model on ER random networks of size N = 2000, 5000 and 10000 nodes, and $\langle k \rangle = 4$. The reason we chose these network configurations was that we want to observe the effects of neighbouring distance d comparing with the average path length $\langle l \rangle$ of the network. With small world effect, we see that $\langle l \rangle$ depends on $\ln N / \ln \langle k \rangle$ (Eq. 2.11). Due to computational resources limitation, we consider N up to 10,000 nodes. However, the network size must be large enough to correspond to the real systems. The smallest size we used is 2,000 nodes. In our work, we consider $\langle k \rangle = 4$, which corresponds to $\langle l \rangle \approx$ 5.5, 6.1 and 6.6 for N = 2000, 5000 and 10000 nodes respectively. With these configurations, we can observe the dynamics due to small value of d, for example $d = 4$, which is less than the above chosen values of $\langle l \rangle$. Note that d must be greater than two because if a node rewires to its adjacent susceptibles, then its new link will be a double link, which is prohibited from our network.

4.1 Effects of local rewiring method

In this section we present the results of simulating the adaptive SIS on ER random network to explain how the local rewiring affects the epidemic dynamics.

4.1.1 Dynamics on topological networks

Let us first consider the case that there is only local rewiring process ($w_d \neq 0$ but $b = r = 0$). Fig. 4.1 shows that at the beginning, with the fraction of initial infected nodes $[i]_0 = 0.1$, the giant component consists of S-nodes and I-nodes (Fig. 4.1a). As time progresses, I-nodes are isolated from the giant component so the size of the giant component decreases and the number of small components increases (Fig. 4.1b). Eventually, there is no network dynamics when all of I-nodes are separated from the giant component (Fig. 4.1c). In the case of no epidemic dynamics, the fraction of the S-nodes and I-nodes in the network are constant. However, the number of SI-links decreases until S-nodes and I-nodes are totally separated, i.e. $[si] = 0$ (Fig. 4.2).

Fig. 4.3 shows a similar dynamics as that in Fig. 4.1 but with different fraction of initial infected nodes $[i]_0 = 0.9$. The network tends to split up I-nodes from S-nodes. Then S-nodes join together densely and connect loosely to I-nodes (Fig. 4.3b). Eventually, S-nodes and I-nodes are totally separated. In this case, there are two large components (Fig. 4.3c); one is full of I-nodes, and the other, which is larger than the former, consists of S-nodes. The networks are in steady state and there is no rewiring event anymore when $[si] = 0$ (Fig. 4.4).

The small components whose S-nodes and I-nodes tend to avoid SI-links and split into smaller components if they can. The rewiring event cannot happen across components due to the local rewiring rule. Thus, the giant component will become smaller and smaller until there is no dynamics in its component. If the epidemic dynamics is switched on, the dynamics in the small components will stop when all nodes are susceptible whereas the dynamics of the giant component depends on the rates of b and w. In this regard, the dynamics of small components are trivial. Henceforth, without loss of generality, we study only the giant component instead of the whole network.

To investigate how the neighbouring distance d affects to the dynamics, we consider the fraction of infected nodes in the giant component $[i_g]$ for various

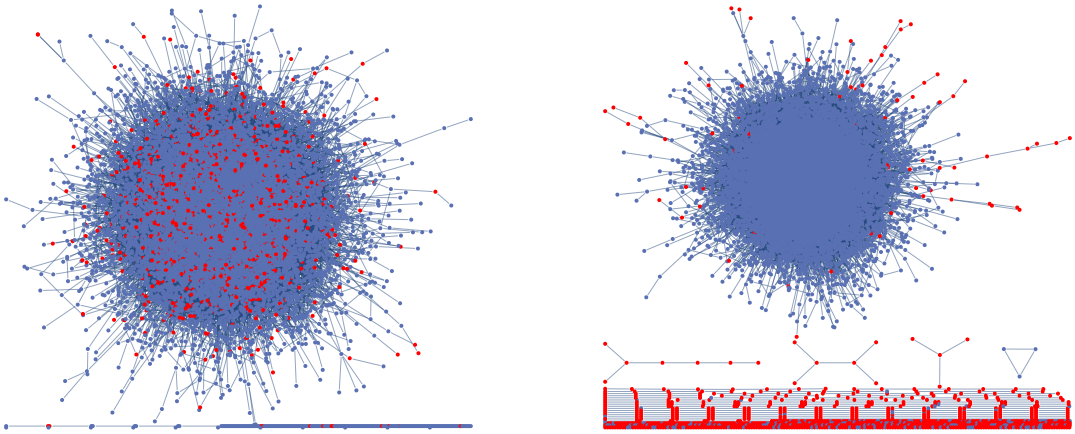

(a) (b)

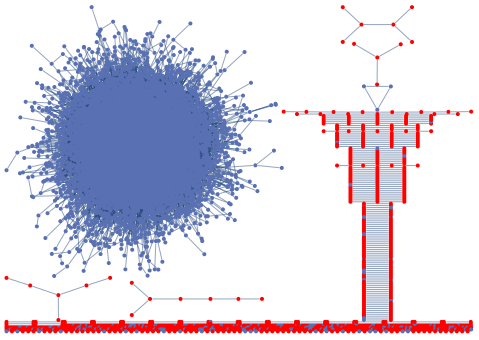

(c)

Figure 4.1: Snapshots of adaptive SIS epidemic network with local rewiring and without epidemic dynamics. The initial infected fraction is 0.1. S-nodes are represented by blue dots and I-nodes are represented by red dots. a) At initial time $t = 0\ w_d^{-1}$, the fraction of the giant component is 0.98. b) At $t = 1\ w_d^{-1}$, the fraction of the giant component is 0.89. c) At $t = 1,000\ w_d^{-1}$, the fraction of the giant component is 0.88. The plots correspond to $N = 10^4, \langle k \rangle = 4, b = r = 0, w_d \neq 0$ and $d = 4$.

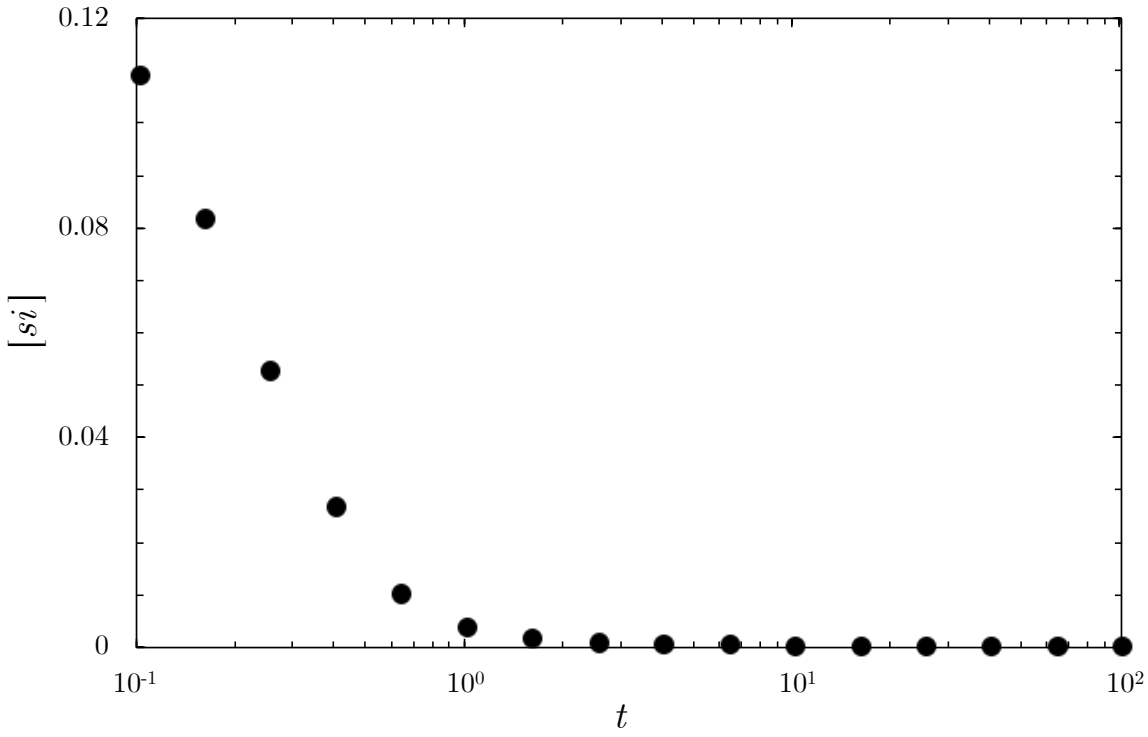

Figure 4.2: Fraction of SI-links $[si]$ as a function of time. The parameters are chosen to be the same as in Fig. 4.1. The results of simulations are averaged over 100 trials.

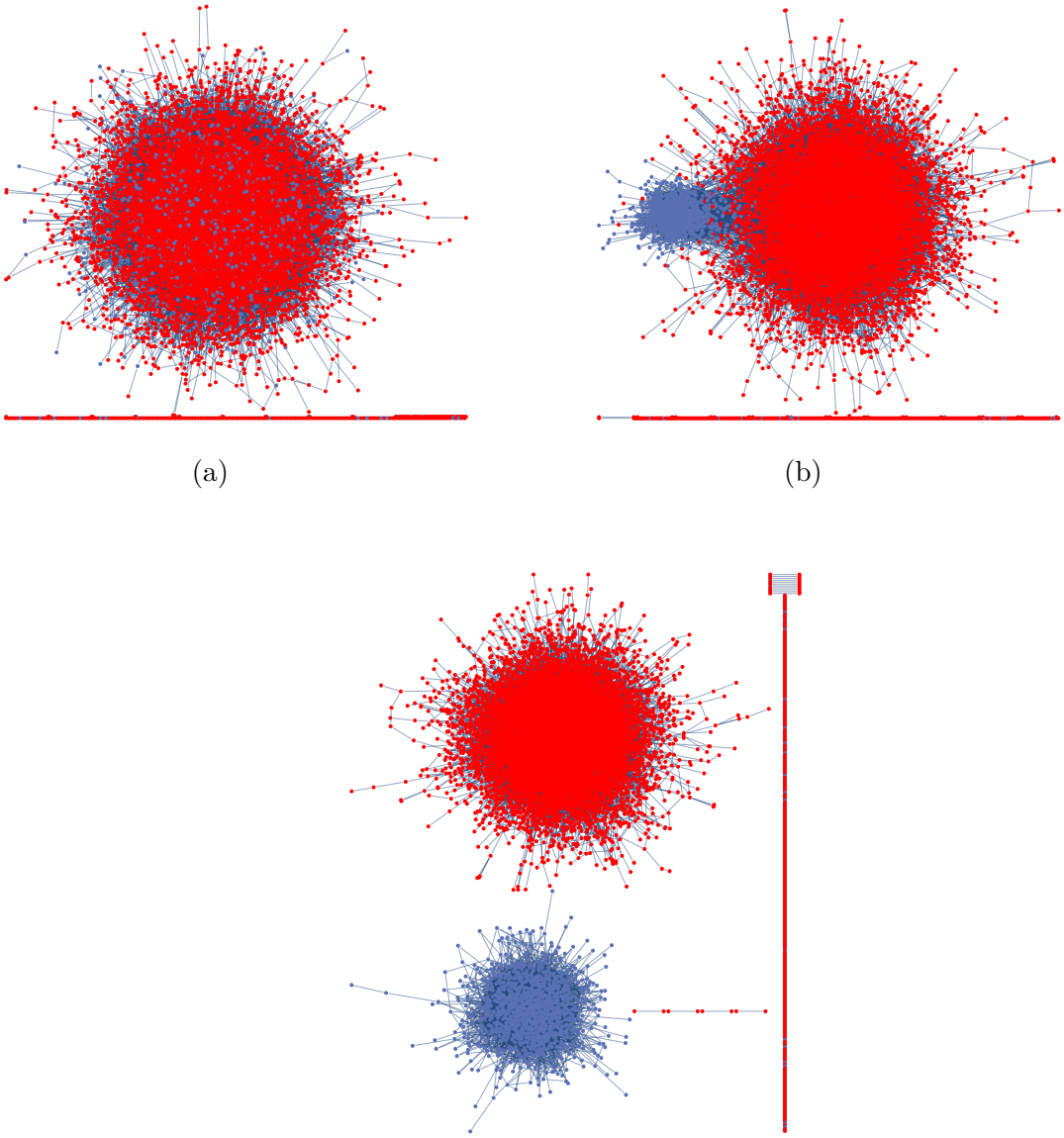

(a) (b)

(c)

Figure 4.3: Snapshots of adaptive SIS epidemic network with local rewiring and without epidemic dynamics. The initial infected fraction is 0.9. S-nodes are represented by blue dots and I-nodes are represented by red dots. a) At initial time $t = 0\ w_d^{-1}$, the fraction of the giant component is 0.98. b) At $t = 1\ w_d^{-1}$, the fraction of the giant component is 0.97. c) At $t = 1,000\ w_d^{-1}$, the fraction of the giant component is 0.87. The plots correspond to $N = 10^4, \langle k \rangle = 4, b = r = 0, w_d \neq 0$ and $d = 4$.

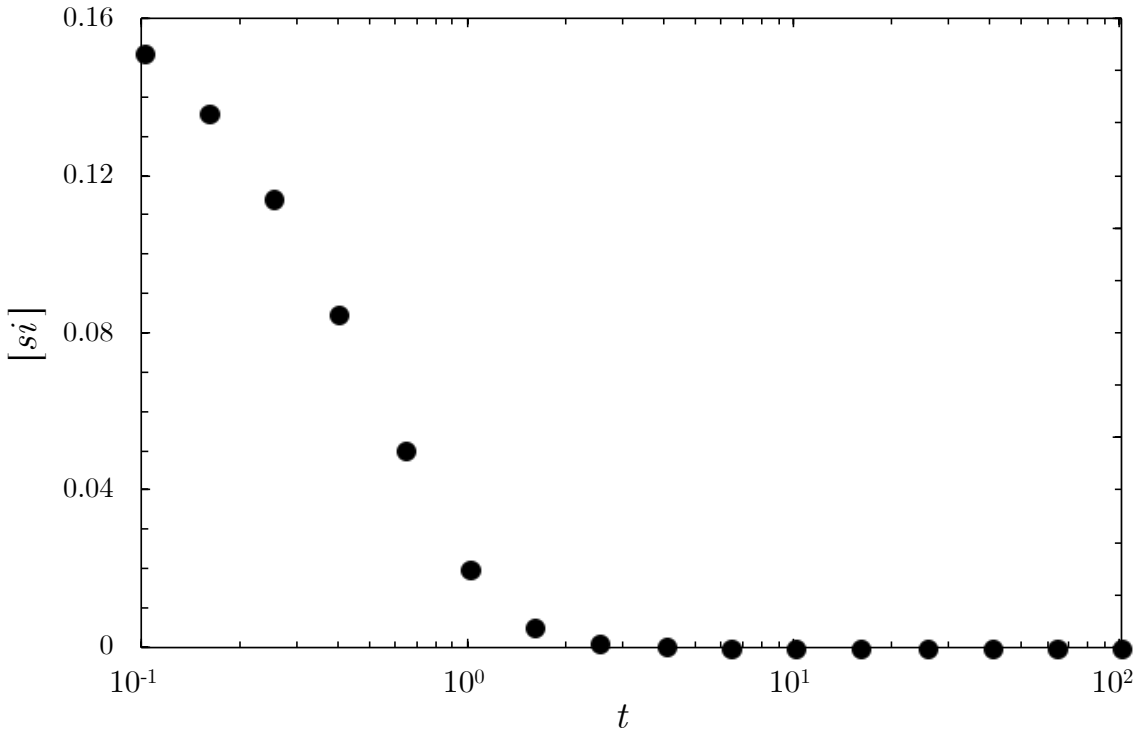

Figure 4.4: Fraction of SI-links $[si]$ as a function of time. The parameters are chosen to be the same as in Fig. 4.3. The results of simulations are averaged over 100 trials.

values of d comparing to the average path length in the giant component $\langle l \rangle$. We simulate the network size of $N = 10^4$ and $\langle k \rangle = 4$ so $\langle l \rangle \simeq 6.7$. We consider $d = 4, 8$ and ∞. Fig. 4.5 shows that $[i_g]$ decreases faster when $d > \langle l \rangle$ than $d < \langle l \rangle$. This is not surprising because larger d means higher chance to rewire. However, at very large d, i.e. $d = \infty$, the ability to prevent infection is not different from $d \gtrsim \langle l \rangle$ because at that stage, information about a node is know throughout the whole graph.

4.1.2 Epidemic dynamics with local rewiring

Now we consider the case with both epidemic dynamics and local rewiring. We begin with the simulations of networks in disease-free phase with $b = 1, w_d = 6$ and $d = 4$ shown in Fig. 4.6. At time $t = 0$, the ER network consists of one giant component and some small components (Fig. 4.6a). As time progresses, with local rewiring mechanism S-nodes attempt to avoid infection by rewiring from I-neighbouring nodes to other S nodes, and then the I-nodes are isolated from the giant component. In Fig. 4.6b at time $t = 1$, there are many small components of I-nodes, separated from the giant components where as the giant component contains compact group of S-nodes and loose group of I-nodes. At $t = 100$, all nodes in the giant component are S-nodes (Fig. 4.6c), then the network reaches its steady state. Along the network evolution, size of giant component is reduced and the number of small components increases as shown in Fig. 4.7. As we discuss above, because of the local rewiring mechanism, the separated recovered nodes cannot reconnect to the giant component. Fig. 4.8 confirms that in this case the local rewiring method can also prevent infection by splitting I-node from the giant component using only information about the nearby neighbourhood other than global information as in the global rewiring method [53].

The effect of local rewiring on the network structure is further described in Fig. 4.9. With the local rewiring, the average degree of the giant component k_g tends to increase. This is because there are some nodes separated from the giant

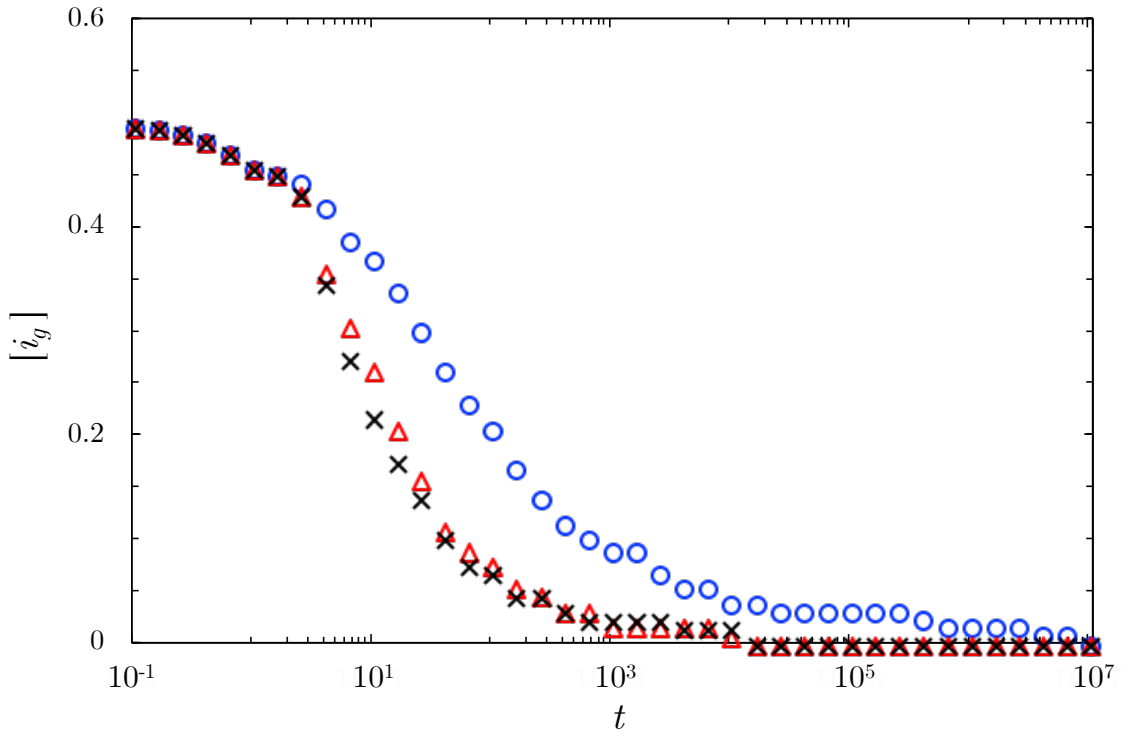

Figure 4.5: Fraction of infected nodes in the giant component $[i_g]$ as a function of time. Simulations are performed for adaptive SIS on ER networks without epidemic dynamics ($b = r = 0$) with $N = 10^4, \langle k \rangle = 4, [i]_0 = 0.5$ and $w = 6$ for various d: $d = 4$ (blue circle), $d = 8$ (red triangle) and $d = \infty$ (black x-cross).

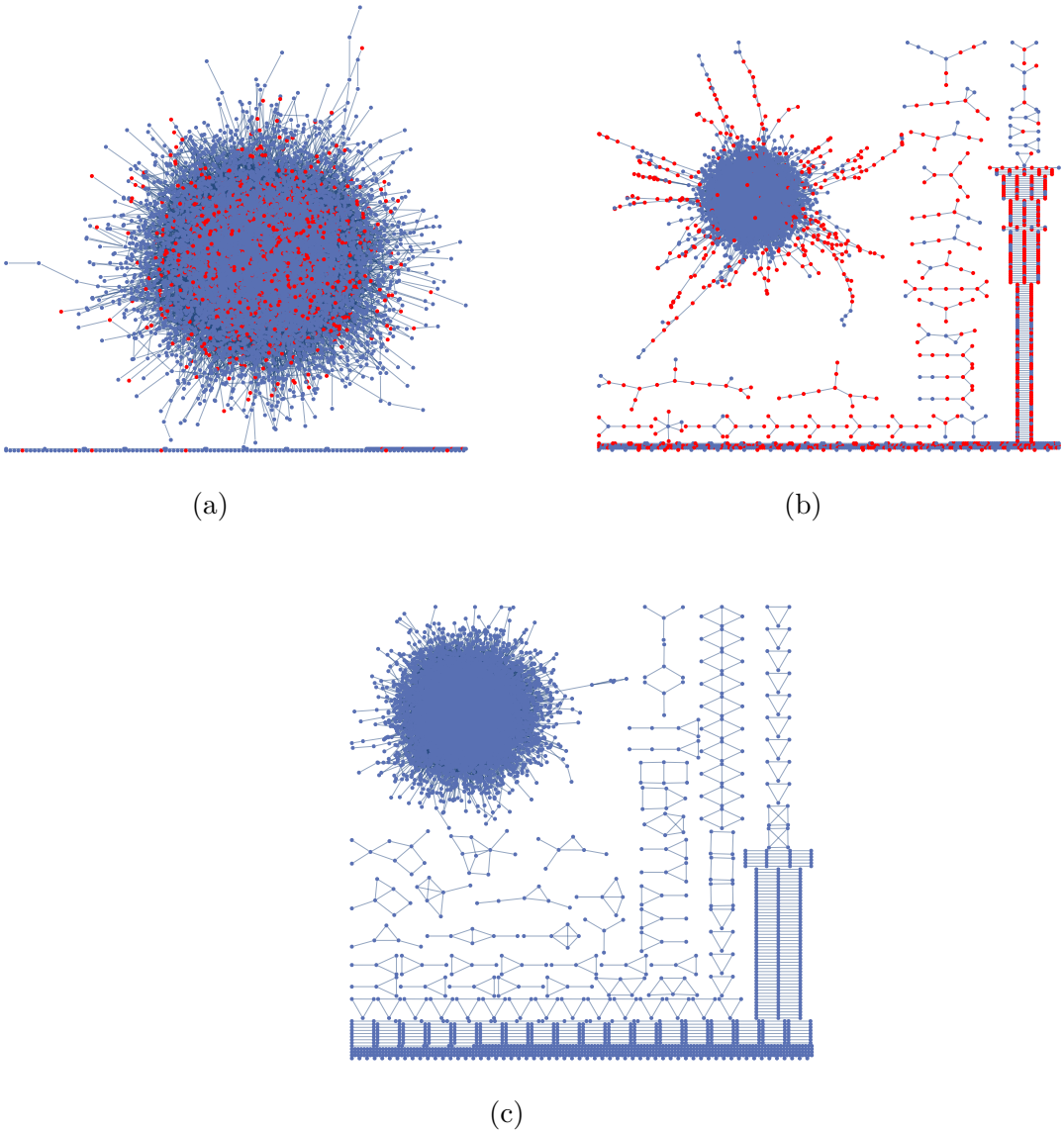

(a) (b)

(c)

Figure 4.6: Snapshots of adaptive SIS epidemic network with local rewiring in disease-free phase with S-nodes (blue) and I-nodes (red). a) At initial time $t = 0$ r^{-1}, the fraction of the giant component is 0.98. b) At $t = 1$ r^{-1}, the fraction of the giant component is 0.9. c) At $t = 100$ r^{-1}, the fraction of the giant component is 0.84. The plots correspond to $N = 10^4, \langle k \rangle = 4, [i]_0 = 0.1, b = 1$, $w_d = 6$ and $d = 4$. Figure reprinted from [49].

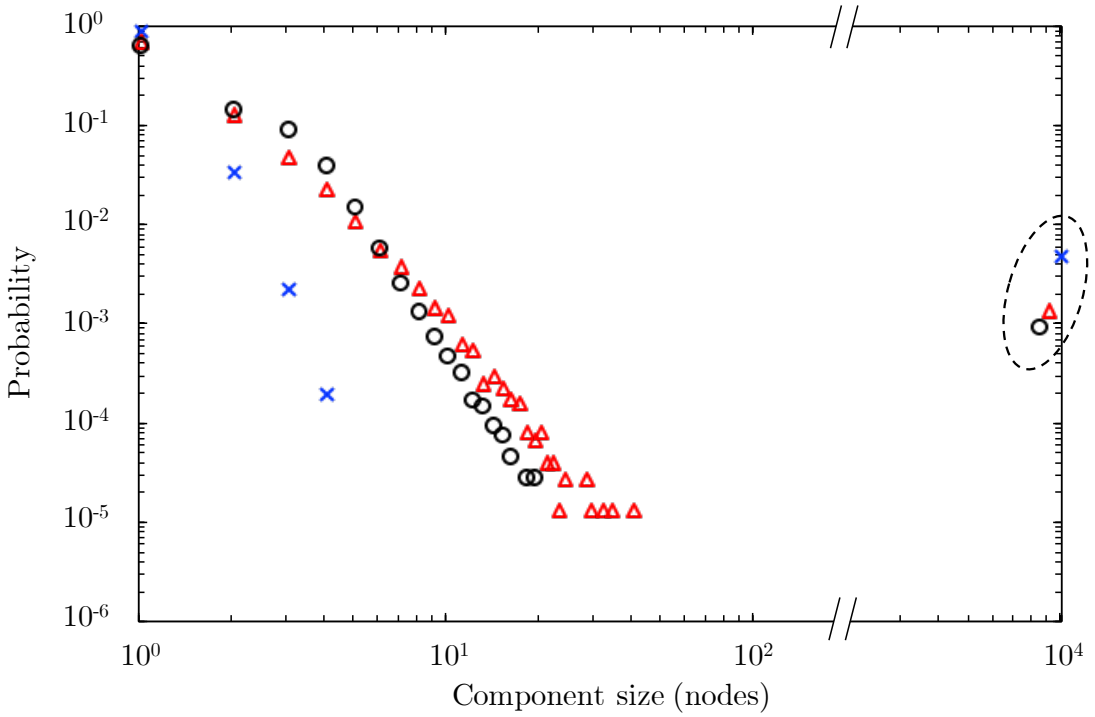

Figure 4.7: Distribution of component sizes of adaptive SIS epidemic network with local rewiring in disease-free phase at $t = 0\ r^{-1}$ (blue x-crosses), $t = 1\ r^{-1}$ (red triangles) and $t = 100\ r^{-1}$ (black circles). The plots in the dashed circle represent for the giant component. The parameters are chosen to be the same as in Fig. 4.6. The results of simulations are averaged over 100 trials. Figure reprinted from [49].

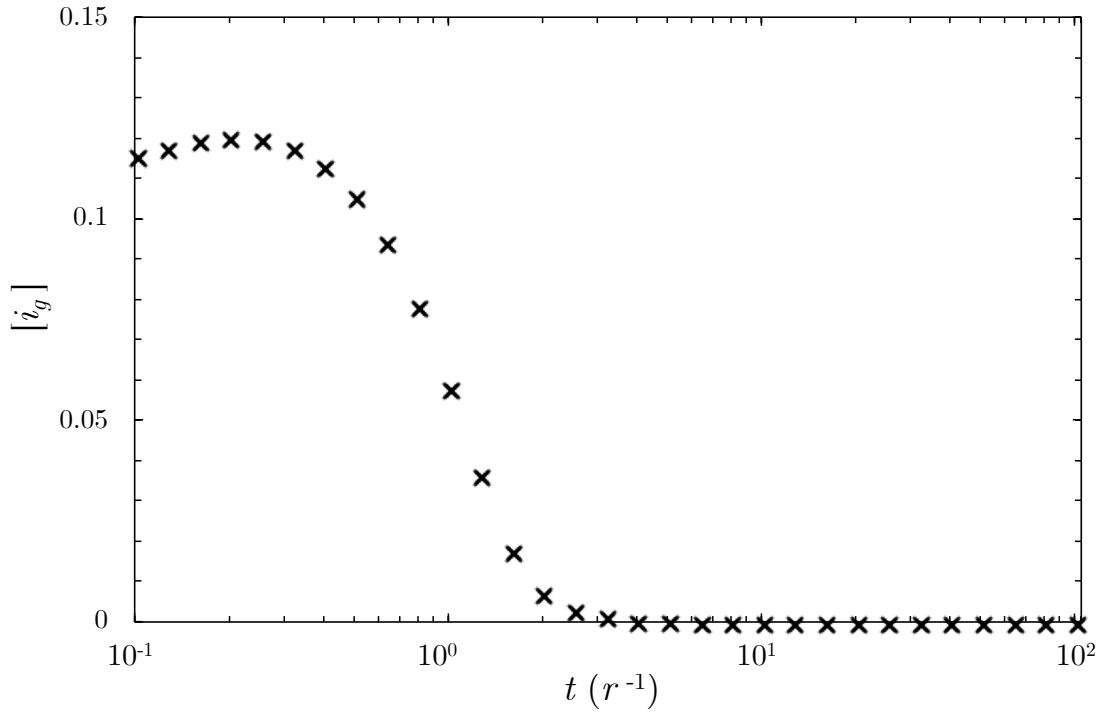

Figure 4.8: Fraction of infected nodes in the giant component $[i_g]$ as a function of time. Simulations are performed for adaptive SIS epidemic network in disease-free phase with parameters chosen to be the same as in Fig. 4.6. The results of the simulations are averaged over 100 trials. Figure reprinted from [49].

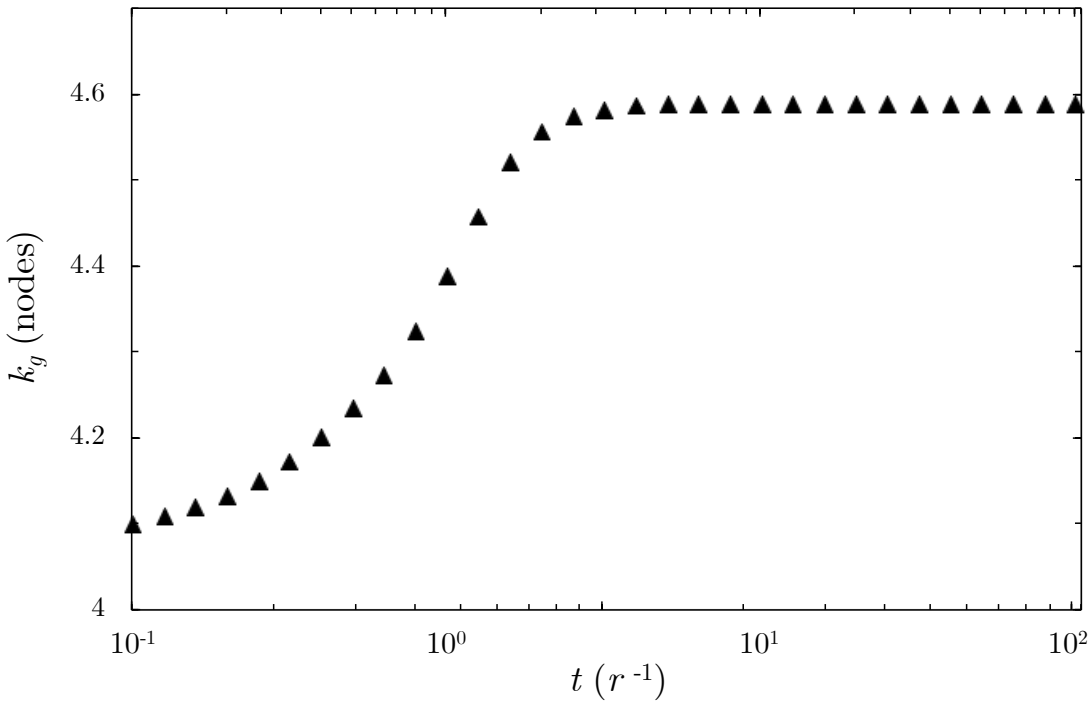

Figure 4.9: Average degree of nodes in the giant component (k_g) as a function of time. Simulations are performed for adaptive SIS epidemic network in disease-free phase with parameters chosen to be the same as in Fig. 4.6. The results of simulations are averaged over 100 trials. Figure reprinted from [49].

component due to breaking of SI-links. However, the total number of degrees in the giant component does not quite decrease because S-nodes create SS-links substituting the broken SI-links within the component. The value of k_g is constant when there are only S-nodes in the giant component, i.e., the network is in the disease-free phase. Degree distribution in the giant component in Fig. 4.10 shows that the degree distributions of both S-nodes and I-nodes are broadened from the initial profile. This is because S-nodes increase their degrees by rewiring to other S-nodes whereas the I-nodes has broadened because of the new infections in the susceptible group. Furthermore, the mean degree of S-nodes increases whereas the mean degree of I-nodes decreases.

Next we consider networks in endemic phase with $b = 1, w_d = 2$ and $d = 4$ shown in Fig. 4.11. In this case, rewiring is not fast enough to separate I-nodes and S-nodes completely. However, the rewiring mechanism tries to form two loosely connected groups of S-nodes and I-nodes (Fig 4.11b). While SI-links are continuously broken by rewiring, new S-nodes are created by recoveries in the infected groups and new I-nodes are created by infections in the susceptible groups (Fig 4.11c). At large time, the local rewiring method is not successful in isolating I-nodes from the giant component so the network is in the endemic phase (Fig 4.11d). As time progresses, the giant component size decreases and many small components of size one are produced shown in Fig. 4.12.

For long-time evolution, $[i_g]$ increases continuously (Fig. 4.13). The value of $[i_g]$ will tend to constant ($[i_g] > 0$) when there is no chance for nodes in the giant component to rewire anymore. It means that there is only dynamics of states and the network is in the endemic phase. In this network, the effect of local rewiring to the network structure is more apparent than that of the previous one. The value of k_g in Fig. 4.14 continues to increase. Eventually k_g is more than double its initial value. Note that we do not show the plot of k_g as a function of time from the beginning until steady state. Because the steady state occurs at very large time ($t \sim 10^9$) and tracking the network structure throughout the whole history is very time consuming. So we simulate the networks and let them evolve, until very

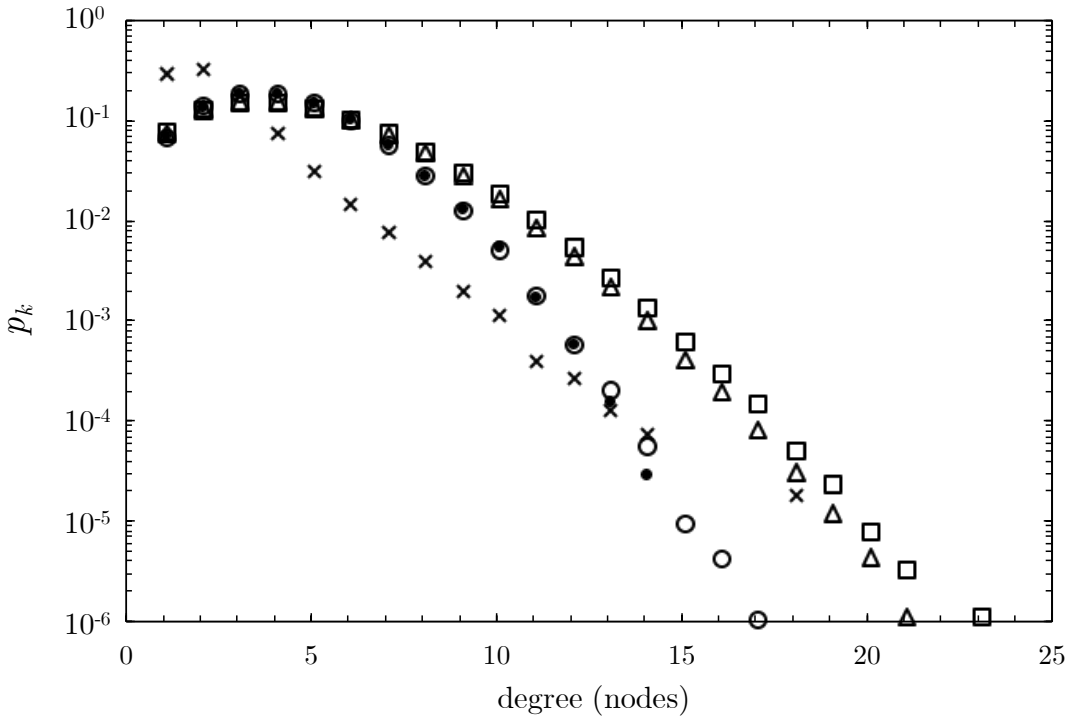

Figure 4.10: Degree distribution in the giant component p_k of adaptive SIS epidemic network with local rewiring in disease-free phase for S-nodes at $t = 0\ r^{-1}$ (circles), $t = 1\ r^{-1}$ (triangles) and $t = 100\ r^{-1}$ (squares) and I-nodes at $t = 0$ r^{-1} (dots) and $t = 1\ r^{-1}$ (crosses). The average degrees of S-nodes in the giant component are 4.1, 4.5 and 4.6 for $t = 0, 1$ and 100 respectively. The average degrees of I-nodes in the giant component are 4.1 and 2.3 for $t = 0$ and 1, respectively. The parameters are chosen to be the same as in Fig. 4.6. The results of simulations are averaged over 100 trials. Figure reprinted from [49].

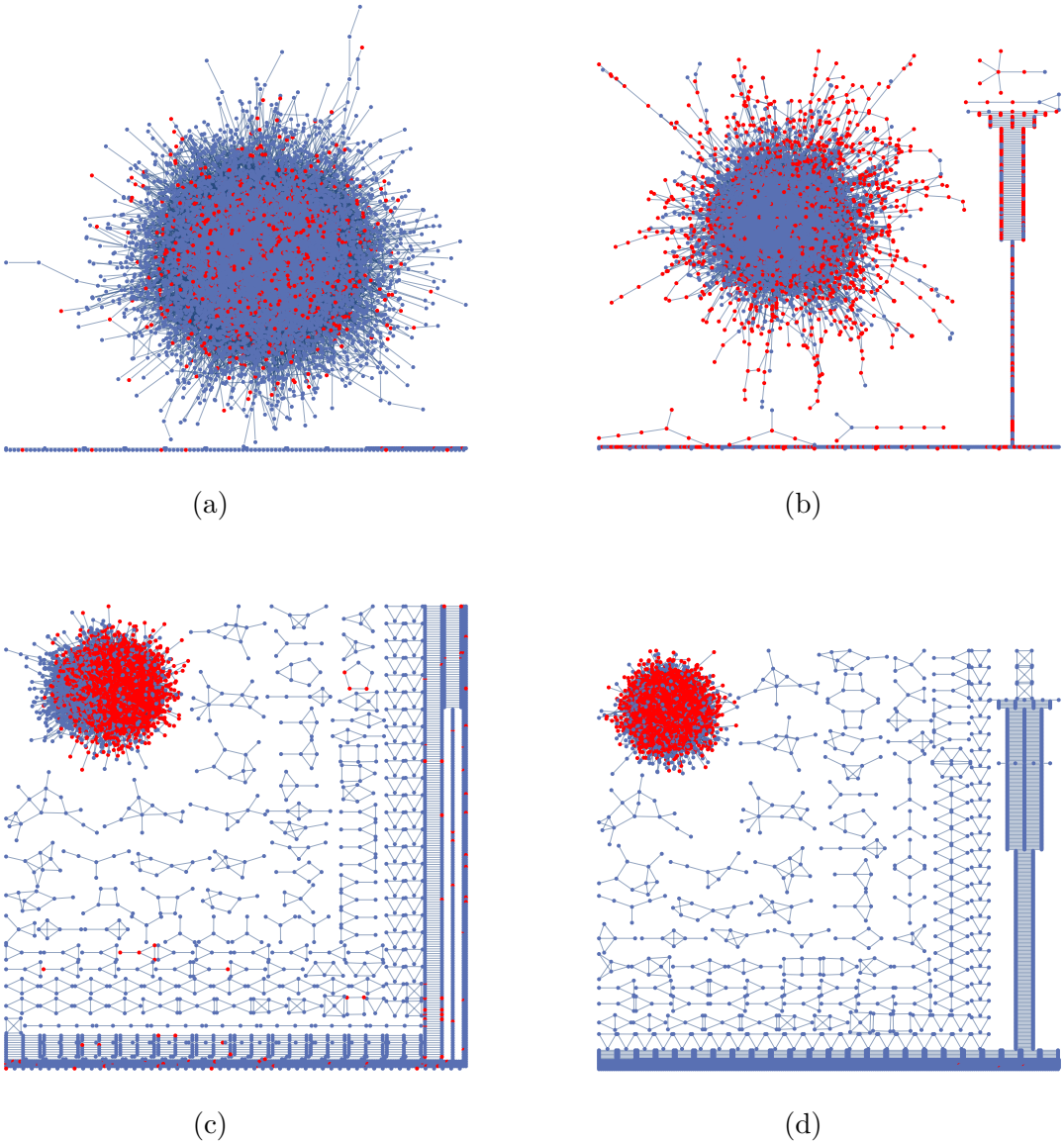

(a) (b)

(c) (d)

Figure 4.11: Snapshots of adaptive SIS epidemic network with local rewiring in endemic phase with S-nodes (blue) and I-nodes (red). a) At initial time $t = 0$ r^{-1}, the fraction of the giant component is 0.98. b) At $t = 1$ r^{-1}, the fraction of the giant component is 0.97. c) At $t = 10$ r^{-1}, the fraction of the giant component is 0.9. d) At $t = 100$, the fraction of the giant component is 0.72. The plots correspond to $N = 10^4, \langle k \rangle = 4, b = 1$ and $w_d = 2$. Figure reprinted from [49].

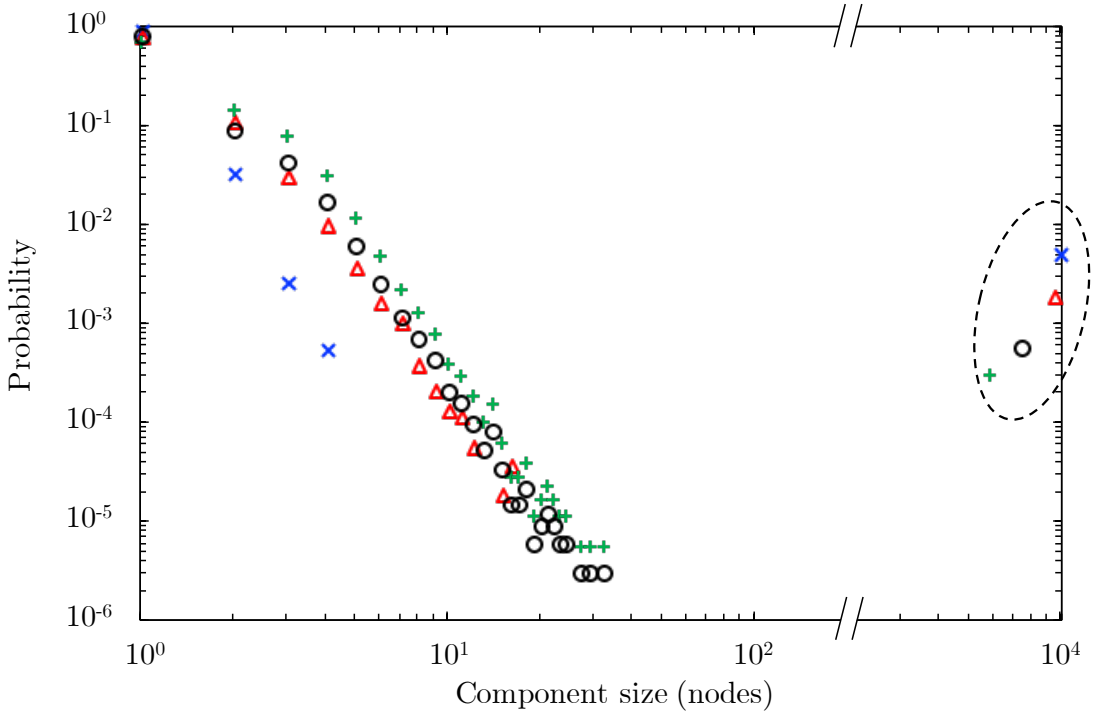

Figure 4.12: Distribution of component sizes of adaptive SIS epidemic network with local rewiring in endemic phase at $t = 0\ r^{-1}$ (blue x-crosses), $t = 1\ r^{-1}$ (red triangle), $t = 10\ r^{-1}$ (black circle) and $t = 100\ r^{-1}$ (green crosses). The marks in the dashed circle represent for the giant component. The parameters are chosen to be the same as in Fig. 4.11. The results of simulations are averaged over 100 trials. Figure reprinted from [49].

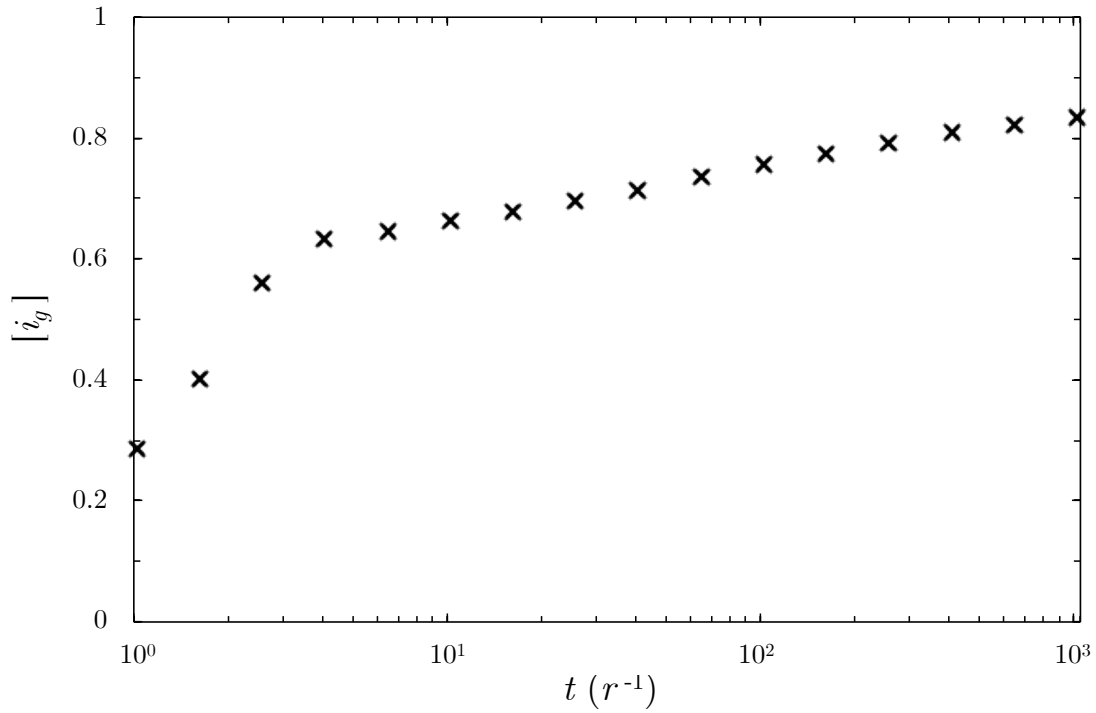

Figure 4.13: Fraction of infected nodes in the giant component $[i_g]$ as a function of time. Simulation are performed for adaptive SIS epidemic network in endemic phase with parameters chosen to be the same as in Fig. 4.11. The results of simulations are averaged over 100 trials. Figure reprinted from [49].

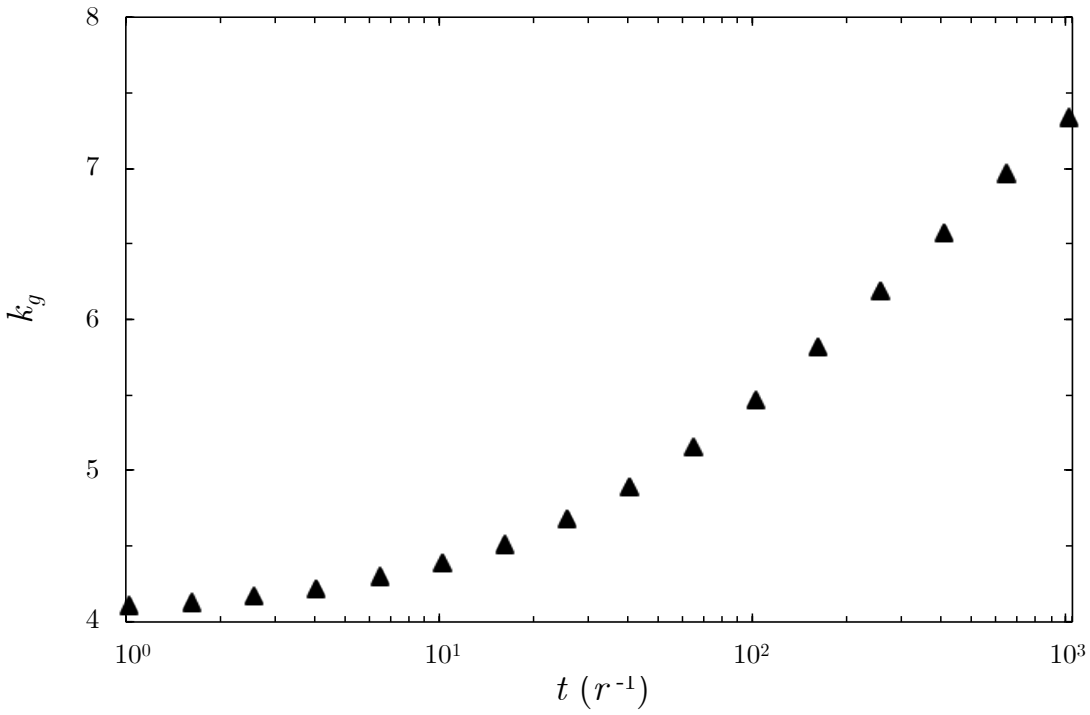

Figure 4.14: Average degree of nodes in the giant component (k_g) as a function of time. Simulation are performed for adaptive SIS epidemic network in endemic phase with parameters chosen to be the same as in Fig. 4.11. The results of simulations are averaged over 100 trials. Figure reprinted from [49].

large time before we start to observe the network structure. As an example, we plot time evolution of k_g for small networks size ($N = 500$) as shown in Fig. 4.15. This plot illustrates that k_g increases slowly at the beginning, after that it grows rapidly until reaching a constant value at steady state. The degree distributions of $N = 10^4$ are shown in Fig. 4.16. In the case of endemic phase, distributions for both I-nodes and S-nodes are broadened corresponding to the increasing value of k_g. The average degree tends to increase. Moreover, the average degree of I-nodes is a bit higher than the average degree of S-nodes. So disease transmission is highly likely.

4.1.3 Summary

Results in this section are summarised as follows. With the local rewiring mechanism, I-nodes are isolated from the giant component. This process makes the size of the giant component decreases and the number of the small components increases. However, the network still contains one largest component and the dynamics of network depends on this component. That is the reason why we only study the giant component instead of the whole network. We already show that the local rewiring can prevent infections by using less information than can the global rewiring. However, the effects of local rewiring may give the opposite result. Due to the high connectivity within the giant component, the infection among the group of S-nodes is easy to disperse.

4.2 Bifurcation diagrams

In this section, we will show how steady-state solutions of infected fraction $[i_g]_f$ depend on the value of d. Our simulations are performed with $N = 2000$, $\langle k \rangle = 4$ and $w = 2$ so at initial time $\langle l \rangle \simeq 5.6$. In Fig. 4.17 the analytical results from the pair approximation model, calculated from Eqs. 3.6, are compared with numerical simulations of the full adaptive SIS model at $d = 4$. Let us first consider the

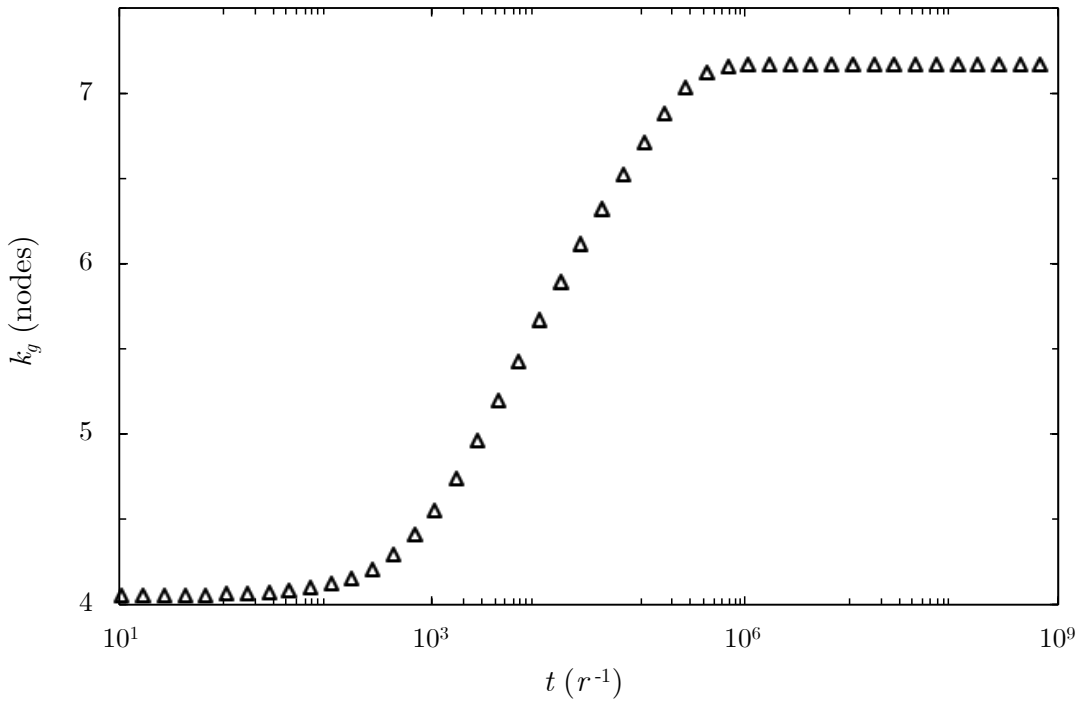

Figure 4.15: Average degree of nodes in the giant component (k_g) as a function of time. The plots correspond to $N = 500, \langle k \rangle = 4, b = 0.5$ and $w_d = 0.1$. The results of simulations are averaged over 200 trials. Figure reprinted from [49].

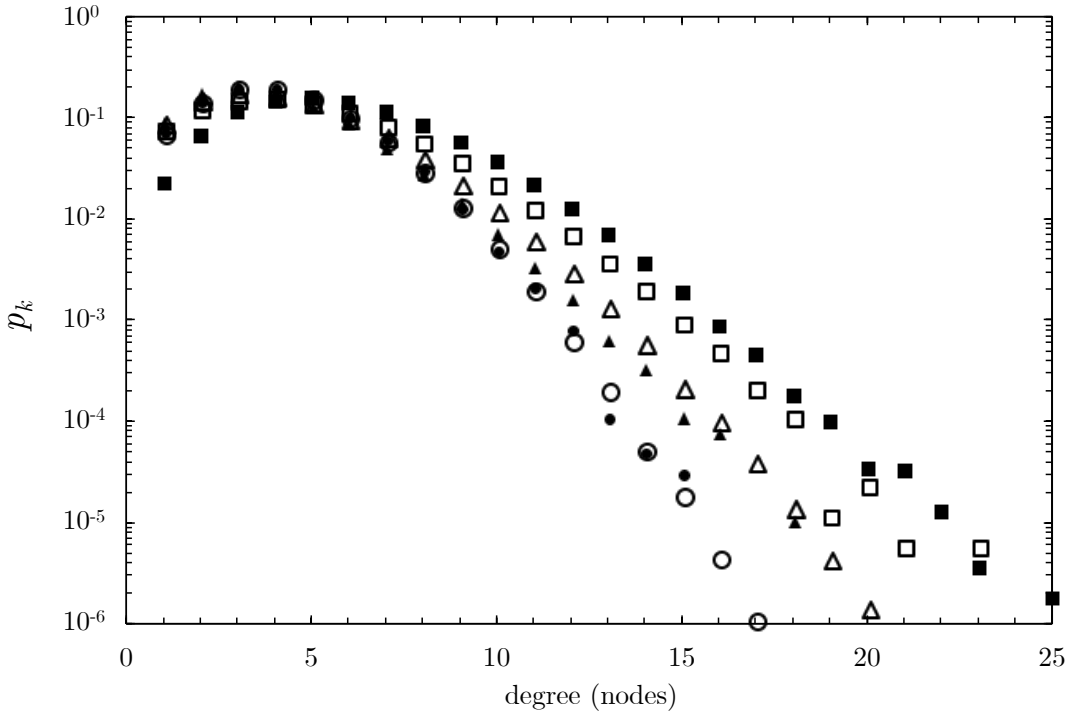

Figure 4.16: Degree distribution in the giant component p_k of adaptive SIS epidemic network with local rewiring in endemic phase for S-nodes at $t = 0\ r^{-1}$ (circles), $t = 1\ r^{-1}$ (triangles) and $t = 100\ r^{-1}$ (squares) and I-nodes at $t = 0\ r^{-1}$ (dots), $t = 1\ r^{-1}$ (solid triangles) and $t = 100\ r^{-1}$ (solid squares). An average degree of S-node in the giant component are = 4.1, 4.2 and 4.8 for $t = 0$, 1 and 100, respectively. An average degree of I-node in the giant component are 4.1, 3.9 and 5.7 for $t = 0$, 1 and 100, respectively. The parameters are chosen to be the same as in Fig. 4.11. The results of simulations are averaged over 100 trials. Figure reprinted from [49].

numerical results. When epidemic dynamic is switched on, i.e. $b > 0$, we found two thresholds. The first one is the epidemic threshold where the network changes from disease-free phase ($[i_g]_f = 0$) to endemic phase ($[i_g]_f > 0$). The second one is the persistence threshold where the network transitions from the endemic phase to the disease-free phase. For analytical results, we obtain the solutions of $[i_g]_f$ from computing Eqs. 3.6 at steady state. With the local rewiring, the degree of the giant component k_g is not constant but always increases until reaching its steady state value. As shown in the previous section, in the disease-free phase, k_g does not quite change from $\langle k \rangle$ whereas, in the endemic phase, k_g is much greater than $\langle k \rangle$. In the case of endemic phase, steady state occurs after a very long time as shown in Fig. 4.15. Therefore, the analytical solutions depend on what phase the network is in. In the Fig. 4.17, the lower thick line comes from the solutions in disease-free phase where as the upper thick line comes from the solutions in endemic phase.

The analytical results agree well with the simulation results for value of $[i_g]_f$ but the thresholds occur differently. This is because the approximation of the local rewiring term in Eqs. 3.6. From Eq. 3.4 and the fact that $\langle k \rangle^d$ may exceed the size of the giant component, we approximate $N_d = N_g$ (Eq. 3.5). However this approximation is an overestimation for networks in disease-free phase with small $\langle k \rangle$ and small d, e.g. for the network in Fig. 4.17 where $N_d \approx 4^4 = 256$ which is considerably less than the network size $N = 2,000$. Beside that, in the Eqs. 3.6, the triplets $[SSI]$ and $[ISI]$ are approximated to products of lower moments (Eqs. 2.21). This pair approximation applies well to the global rewiring whose topology is claimed to be random-graph like [37]. For the local rewiring, degree distribution of the giant component is very broad (Fig. 4.10 and 4.16) and the pair approximations for $[SSI]$ and $[ISI]$ overestimates the actual number of triplets. Moreover, the effect of the local rewiring on the network topology is more subtle than that of the global rewiring. Simulation results also depend on the network size. For larger N, at the same value of w_d, the invasion of new disease can occur at lower rate of b. We will discuss this effect in the next section.

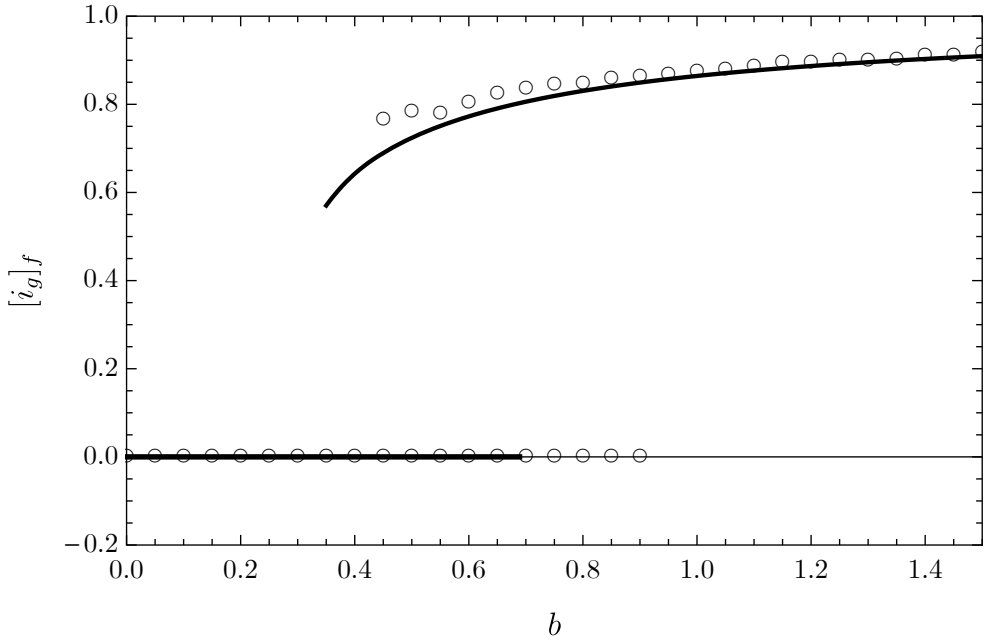

Figure 4.17: Bifurcation diagram for infected density in adaptive SIS epidemic network with local rewiring as a function of infection rate b for $d = 4$ (circles) comparing with analytical results from Eqs. 3.6 (thick lines). The plots correspond to $N = 2\,000, \langle k \rangle = 4$ and $w_d = 2$. The results of simulations are averaged over 10 networks trials for each initial infected fraction $[i]_0 = 0.01, 0.1, 0.9, 0.99$. Figure reprinted from [49].

Now we consider the effect of local and global rewirings to the epidemic and persistence thresholds. For the local rewiring, we simulate networks with three values of d: small value at $d = 4$, large value at $d = 8$ and very large value at $d = \infty$. Fig. 4.18 shows that the different values of d affect the locations of the threshold. For the epidemic threshold, when $d > \langle l \rangle$, the value of threshold is higher than the that of $d < \langle l \rangle$. Comparing with the global rewiring in Fig. 4.19, the epidemic threshold of the networks with large d occurs at the same b as that of the global rewiring. For the persistence threshold, at large d, the value of threshold is also higher than that of small d because nodes have higher chance to rewire. However, even if d is very large, the persistence threshold is still lower than the global rewiring due to the rewiring rules discussed above.

4.3 Phase diagram

The possible asymptotic behaviours of our model can be represented in a phase diagram on the two-dimensional parameter (b, w) as shown in Fig. 4.20. In this diagram we also plot the phase diagram of the global rewiring for comparison. For each rewiring, the diagram is divided into three regions: endemic phase (right-most region for large b), disease-free phase (left-most region for small b), and bistable phase (central region between endemic and disease-free phases). In the bistable phase, the network can be stable in either endemic state or in disease-free state. Fig. 4.20 shows that boundary between endemic and bistable phases for both rewirings are hardly different so the global and local rewirings have similar endemic phase (orange colour). While the boundary between disease-free and bistable phases of the local rewiring (solid triangles) is higher than the global rewiring (solid circles). Thus, there are some overlaps of disease-free phase (blue colour), and bistable (pink colour). This phase diagram is truly remarkable since we can predict outcomes of an epidemic by using only local information.

Fig. 4.21 shows the effect of network size to the values of thresholds. For small b, the values of epidemic and persistence thresholds are quite similar for

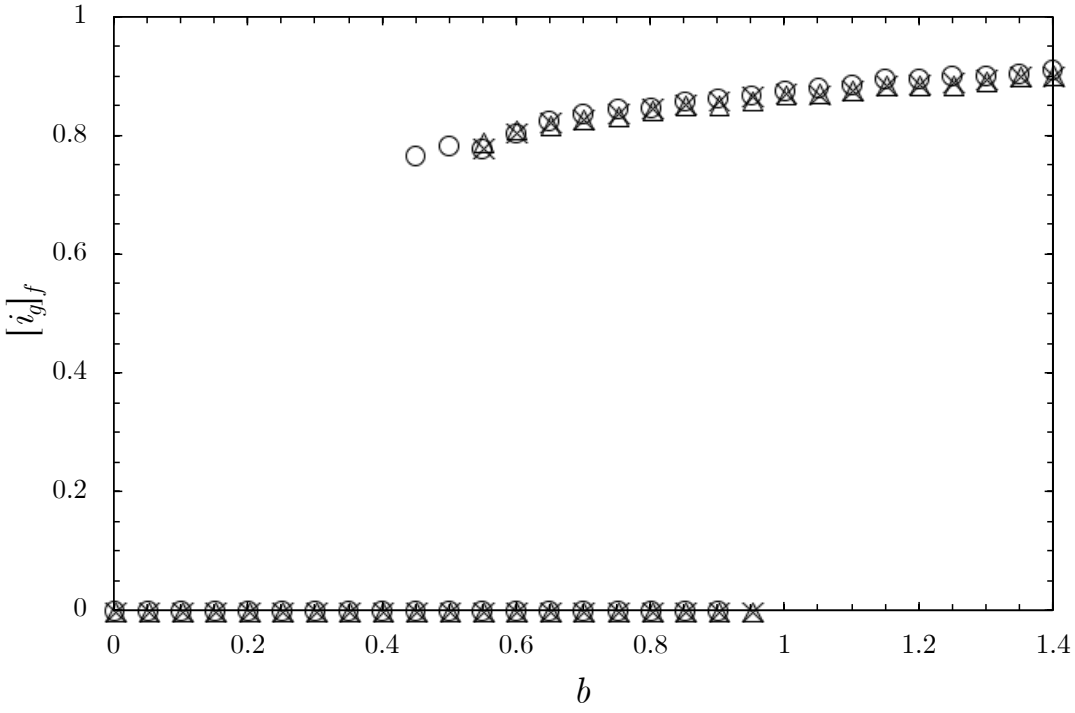

Figure 4.18: Bifurcation diagram for infected density in adaptive SIS epidemic network with local rewiring as a function of infection rate b for different neighbouring distances $d = 4$ (circles), 8 (triangles) and ∞ (crosses). The plots correspond to $N = 2\,000, \langle k \rangle = 4$ and $w_d = 2$. The results of simulations are averaged over 10 networks trials for each initial infected fraction $[i]_0 = 0.01, 0.1, 0.9, 0.99$. Figure reprinted from [49].

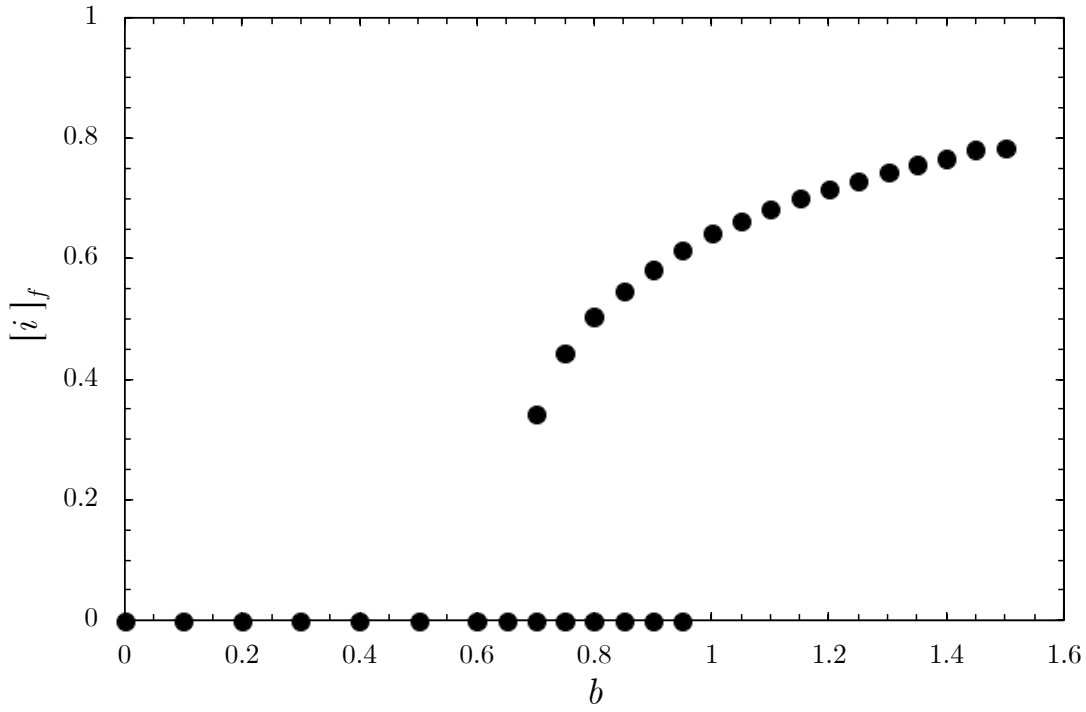

Figure 4.19: Bifurcation diagram for infected density in adaptive SIS epidemic network with global rewiring as a function of infection rate b. The plots correspond to $N = 2\,000, \langle k \rangle = 4$ and $w = 2$. The results of simulations are averaged over 10 networks trials for each initial infected fraction $[i]_0 = 0.01, 0.1, 0.9, 0.99$. Figure reprinted from [49].

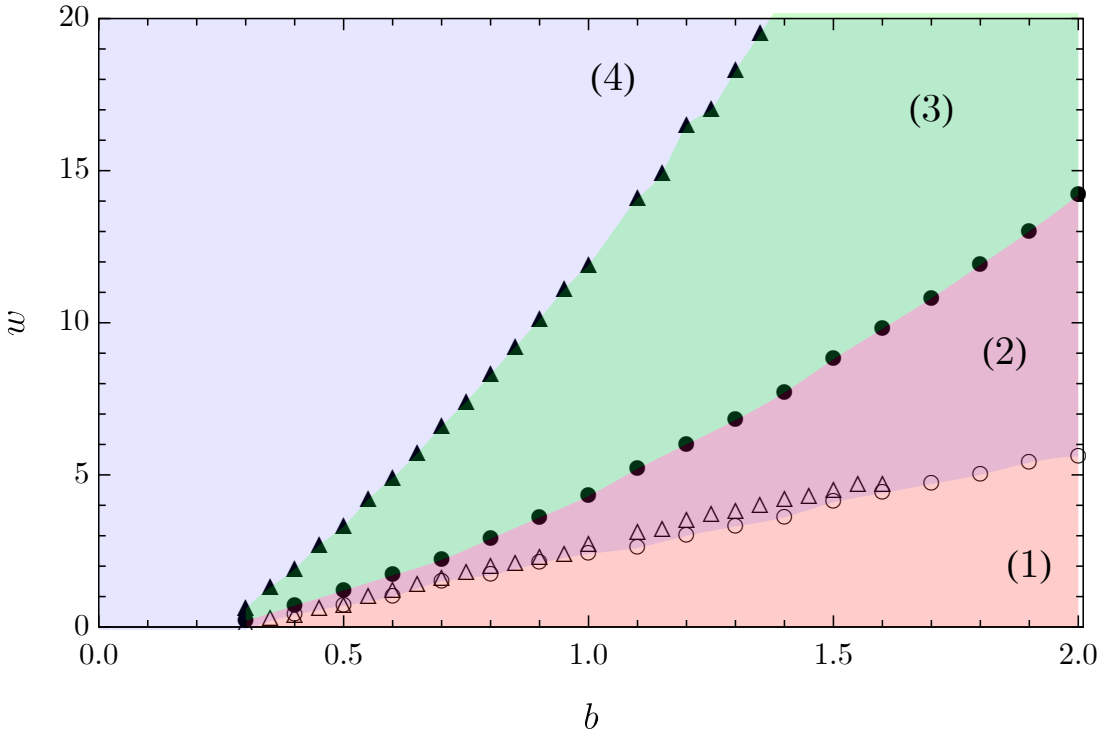

Figure 4.20: Phase diagram of adaptive SIS epidemic network with local rewiring (triangles) and global rewiring (circles). There are some overlap phases between global and local rewirings: (1) endemic phase for both rewirings (orange colour), (2) bistable phase for both rewirings (pink colour), (3) disease-free phase for global rewiring but bistable phase for local rewiring (green colour), and (4) disease-free for both rewirings. The plots correspond to $N = 10^4$ and $\langle k \rangle = 4$ and for the local rewiring $d = 4$. The results of simulations are averaged over 100 trials for each plot. Figure reprinted from [49].

each N. For large b, the thresholds are higher for larger N because the ability of S-nodes to rewire is really restricted to local neighbourhood. Then rewiring event must be fast enough to isolate I-nodes. This means that the effect of local rewiring in large network size is stronger than that of small network size.

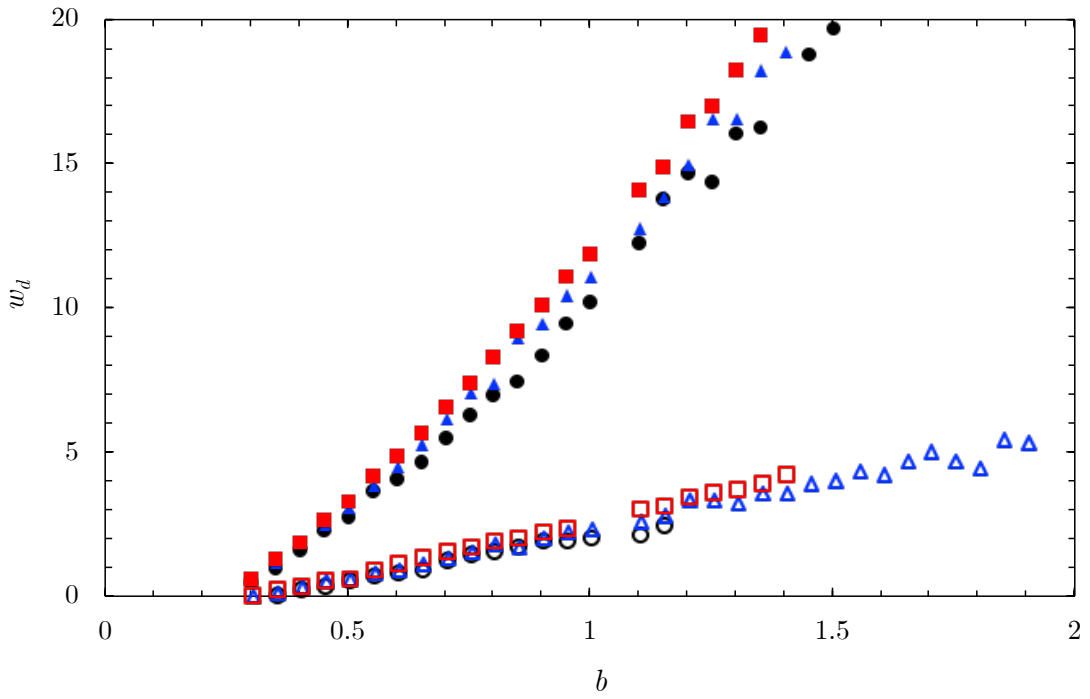

Figure 4.21: Phase diagram of adaptive SIS epidemic network with local rewiring for three network sizes: $N = 2,000$ (circles), $N = 5,000$ (triangles) and $N = 10,000$ (squares). For each N the opened and solid symbols represent, respectively, the epidemic and persistence thresholds. The plots correspond to $\langle k \rangle = 4$ and $d = 4$. The results of simulations are averaged over 100 trials for each plot. Figure reprinted from [49].

CHAPTER V

Conclusions

In this dissertation, we have studied an adaptive SIS epidemic model with the contact-conserving rewiring method on ER model networks. The individuals' decision to avoid infection by changing their social contacts is based completely on information about which epidemiological status the other individuals possess. We replaced the existing rewiring method, the global rewiring that requires information of the entire network, with a more practical rewiring method, the local rewiring, that uses only limited information to make a decision. For controlling real-world diseases, the local rewiring strategy is more suitable since it requires less information than does the global rewiring. The goal of this work is to investigate the effect of local information of the epidemiological status on SIS epidemic spreading in the adaptive network using both continuous-time kinetic Monte Carlo simulations and pair approximation technique.

We have shown that both methods predict similar behaviours. The epidemic threshold and the persistence threshold are obtained with non-zero local rewiring rate $w_d \neq 0$. Although the epidemic thresholds of the global and local rewiring at the same rewiring rate are nearly identical, their persistence thresholds are definitely different. Our results show that there are phase overlaps between both rewiring strategies. This means that under a certain circumstance, we can predict the outcomes of an epidemic for planned interventions. In addition, we compared the efficiency of both rewiring processes in preventing the spread of a disease on the adaptive network. Our results indicate that even with limited local information, we can satisfactorily predict the outcomes of an epidemic.

The impact of neighbouring distance d has been studied on the local rewiring network. With large value of d compared to the average path length of a network, the epidemic threshold and the persistence threshold are higher than the thresholds for small d. As we mentioned, I-nodes are isolated and later they are recovered and have low risk of infection. However, the topological change of the giant component responding to local rewiring is a cause for concern. With the local rewiring, a node cannot rewire across its component to make a connection with another one. So the giant component of S-nodes forms a dense connection which is highly vulnerable to an infection as its size is reduced. Therefore, a small fraction of I-nodes in the giant component which seems to be a little issue may be very difficult to handle since it could cause an epidemic over the component. This situation decreases the effectiveness of targeted vaccination.

Moreover, we have shown that the effect of local rewiring in the network with large size is stronger than that of the network with small size. We conclude that neighbouring distance and network size affect behaviours of the networks, especially the value of the persistence threshold. We have shown that the larger the network size, the lower the persistence threshold. This is because the effect of local rewiring in a large network size is stronger than the effect in a small network size.

Finally, we recommend for further investigation that the pair-approximation should take the triplets or higher-order network structures into account. Since the local rewiring affects the network connections such that the network is strongly localised and makes the prediction of the model less accurate. We suggest that the correlation should be included to the approximation of the triplets. Furthermore, we have studied only the local rewiring on ER random network. With minimal effort, this model should be extended to study more realistic networks with non-Poisson degree distribution.

References

[1] Kermack, W. O., and McKendrick, A. G. A contribution to the mathematical theory of epidemics. *Proc. R. Soc. A* **115** (1927) : 700–721.

[2] Anderson, R. M., and May, R. M. Population biology of infectious diseases: Part I. *Population biology of infectious diseases: Part I* **280** (1979) : 361–367.

[3] Hethcote, H. W., and Yorke, J. A. *Gonorrhea transmission dynamics and control.* Berlin: Springer, Berlin, Heidelberg, 1984.

[4] Brauer, F., and Castillo-Chavez, C. *Mathematical Models in Population Biology and Epidemiology.* 2nd ed. New York: Springer-Verlag New York, 2012.

[5] Brauer, F. Compartmental Models in Epidemiology. in F.Brauer, P.vanden Driessche and J.Wu (ed.), *Mathematical epidemiology*, pp.19–80. Berlin : Springer-Verlag Berlin Heidelberg, 2008.

[6] Albert, R and Barabási, A. Statistical mechanics of complex networks. *Rev. Mod. Phys.* **74** (2002): 47–97.

[7] Newman, M. E. J. Spread of epidemic disease on networks. *Phys. Rev. E* **66** (2002): 016128.

[8] Keeling, M. J. and Eames, K. T. D. Networks and epidemic models. *J. R. Soc. Interface* **2** (2005): 295–307.

[9] Pastor-Satorras, R., Castellano, C., Mieghem, P. V. and Vespignani, A. Epidemic processes in complex networks. *Rev. Mod. Phys.* **87** (2015):925–979.

[10] Gross, T., Dommar D'Lima, C., and Blasius, B. Epidemic dynamics on an adaptive network. *Phys. Rev. Lett.* **96** (2006) : 208701–4.

[11] Funk, S., Salathé, M., and Jansen, V. A. A. Modelling the influence of human behaviour on the spread of infectious diseases: a review. *J. R. Soc. Interface* **7** (2010) : 1247–1256.

[12] Epstein, J. M., Parker, J., Cummings, D., and Hammond, R. A. Coupled contagion dynamics of fear and disease: mathematical and computational explorations. *PLoS ONE* **3** (2008) : e3955.

[13] Omi, S. *SARS – How a global epidemic was stopped* Manila : WHO Regional Office for the Western Pacific, 2006.

[14] Gross, T. and Blasius, B. Adaptive coevolutionary networks: a review. *J. R. Soc. Interface* **5** (2008): 259–271.

[15] Erdős, P. and Rényi, A. On random graphs, I. *Publ. Math. Debrecen* **6** (1959) : 290–297.

[16] Erdős, P. and Rényi, A. On the evolution of random graphs. *Publ. Math. Inst. Hung. Acad. Sci.* **5** (1960) : 17–61.

[17] Erdős, P. and Rényi, A. On the strength of connectedness of a random graph. *Acta Mathematica Academiae Scientiarum Hungaricae* **12** (1961) : 261–267.

[18] Gilbert, E. N. Random Graphs. *Ann. Math. Statist.* **30** (1959) : 1141–1144.

[19] Barabási, A.-L., and Albert, R. Emergence of scaling in random networks. *Science* **286** (1999) : 509–512.

[20] Clauset, A., Shalizi, C.R., and Newman, M. E. J. Power-law distributions in empirical data. *SIAM Review* **51** (2009) : 661–703.

[21] Landau, D. P., and Binder, K. *A guide to Monte Carlo simulations in statistical physics.* Cambridge : Cambridge University Press, 2000.

[22] Newman, M. E. J., and Barkema, G. T. *Monte Carlo methods in statistical physics.* Oxford : Oxford University Press, 1999.

[23] Bulnes, F. M., Pereyra, V. D., and Riccardo, J. L. Collective surface diffusion: N-fold way kinetic Monte Carlo simulation. *Phys. Rev. E* **58** (1998): 86–92.

[24] Serebrinsky, S. A. Physical time scale in kinetic Monte Carlo simulations of continuous-time Markov chains. *Phys. Rev. E* **83** (2011) : 037701.

[25] Barabási, A.-L., and Pósfai, M. *Network Sciences.* Cambridge : Cambridge University Press, 2016.

[26] van Kampen, N. G. *Stochastic process in physics and chemistry.* North-Holland, Amsterdam, 1981.

[27] Castillo-Chavez, C., Feng, Z., and Huang, W. On the computation of Ro and its role on global stability. In C.Castillo-Chavez, S.Blower, P.van den Driessche, D.Kirschner, and A.-A.Yakubu (eds.), *Mathematical approaches for emerging and reemerging infectious diseases: models, methods and theory*, pp. 229–250, New York : Springer-Verlag New York, 2002.

[28] van den Driessche, P., and Watmough, J. Reproduction numbers and subthreshold endemic equilibria for compartmental models of disease transmission. *Math. Biosci.* **180** (2002) : 29–48.

[29] Chowell, G., and Brauer, F. The Basic Reproduction Number of Infectious Diseases: Computation and Estimation Using Compartmental Epidemic Models. in G.Chowell, J.M.Hyman, L.M.A.Bettencourt, and C.Castillo-Chavez (eds.), *Mathematical and Statistical Estimation Approaches in Epidemiology*, pp. 1–30, Dordrecht : Springer, Dordrecht, 2002.

[30] van den Driessche, P., and Watmough, J. Further Notes on the Basic Reproduction Number. In F.Brauer, P.vanden Driessche and J.Wu (ed.), *Mathematical epidemiology*, pp.19–80. Berlin : Springer-Verlag Berlin Heidelberg, 2008.

[31] Newman, M. E. J. *Networks: An Introduction.* New York : Oxford University Press, 2010.

[32] Newman, M. E. J. The structure and function of complex networks. *SIAM Review* **45** (2003) : 167–256.

[33] Fronczak, A., Fronczak, P., and Hołyst, J. A. Average path length in random networks. *Phys. Rev. E* **70** (2004) : 056110.

[34] Newman, M. E. J., Strogatz, S. H., and Watts, D. J. Random graphs with arbitrary degree distributions and their applications. *Phys. Rev. E* **64** (2001) : 026118.

[35] Watts, D. J,. and Strogatz, S. H. Collective dynamics of 'small-world' networks. *Nature* **393** (1998): 440–442.

[36] Strogatz, S. H. Exploring complex networks. *Nature* **410** (2001) : 268–276.

[37] Gross, T. Interplay of network state and topology in epidemic dynamics. In: Boccaletti S, Latora V, Moreno Y (eds) Handbook of biological networks. World Scientific, Singapore, (2009): 417–436

[38] Risau-Gusmán, S. and Zanette, D. H. Contact switching as a control strategy for epidemic outbreaks. *J. Theor. Biol.* **257** (2009): 52–60.

[39] Marceau, V., Noël, P.-A., Hébert-Dufresne, L., Allard, A. and Dubé, L. J. Adaptive networks: Coevolution of disease and topology. *Phys. Rev. E* **82** (2010): 036116.

[40] Shaw, L. B. and Schwartz, I. B. Enhanced vaccine control of epidemics in adaptive networks. *Phys. Rev. E* **81** (2010): 046120.

[41] Schwartz, I. B., Shaw, L. B. and Shkarayev, M. S. Adaptive network dynamics-Modeling and control of time-dependent social contacts. *Proceedings of Fusion* 2011, the 14th International Conference on Information Fusion.

[42] Zanette, D. H. and Risau-Gusmán, S. Infection spreading in a population with evolving contacts. *J. Biol. Phys.* **34** (2008): 135–148.

[43] Taylor, M., Taylor, T. J. and Kiss, I. Z. Epidemic threshold and control in a dynamic network. *Phys. Rev. E* **85** (2012): 016103.

[44] Guo, D., Trajanovski, S., van de Bovenkamp, R., Wang, H. and Mieghem, P. V. Epidemic threshold and topological structure of susceptible-infectious-susceptible epidemics in adaptive networks. *Phys. Rev. E* **88** (2013): 042802.

[45] Rand, D.A. Correlation equations and pair approximations for spatial ecologies. edited by Jacqueline M. McGlade. *CWI Quarterly*, Vol. 12 (3&4), (Centrum Wiskunde & Informatica, Wiley-Blackwell, 1999), p. 329

[46] Zschaler, G. Adaptive-network models of collective dynamics. *Eur. Phys. J. Spec. Top.* **211** (2012): 1–101.

[47] Kiss, I. Z., Miller, J. C. and Simon, P. L. *Mathematics of Epidemics on Networks: From Exact to Approximate Models.* Springer, Switzerland, 2010.

[48] Shaw, L. B. and Schwartz, I. B. Fluctuating epidemics on adaptive networks. *Phys. Rev. E* **77** (2008): 066101.

[49] Piankoranee, S. and Limkumnerd, S. Effects of local rewiring on SIS epidemic adaptive networks. Manuscript submitted for publication.

[50] Allen, L. J.S. An Introduction to Stochastic Epidemic Models. In F.Brauer, P.vanden Driessche and J.Wu (eds.), *Mathematical epidemiology*, pp.81–132. Berlin : Springer-Verlag Berlin Heidelberg, 2008.

[51] Fennel, P. G., Melnik, S. and Gleeson, J. P. Limitations of discrete-time approaches to continuous-time contagion dynamics. *Phys. Rev. E* **94** (2016): 052125.

[52] Van Mieghem, P. *Performance Analysis of Complex Networks and Systems.* Cambridge: Cambridge University Press, 2014.

[53] Piankoranee, S. and Limkumnerd, S. Effects of global and local rewiring in epidemic adaptive networks. *Journal of Physics: Conference Series* **1144** (2018): 012080.

Vitae

Miss Suwakan Piankoranee was born on 24 April 1980 in Bangkok, Thailand. She received her Bachelor degree of Science in Physics from Chulalongkorn University in 1999. She continued studying and received Master's Degree of Science in Physics from Chulalongkorn University in 2004.

Publications:

2018 Piankoranee, S., and Limkumnerd, S. Effects of global and local rewiring on SIS epidemic adaptive networks. (accepted for publication in *Journal of Physics: Conference Series*).

Conference Presentations:

2017 Piankoranee, S., and Limkumnerd, S. Role of mutual information in discrete and continuous time Markov chains. Siam Physics Congress 2017, Rayong, Thailand (24-26 May 2017).

2018 Piankoranee, S., and Limkumnerd, S. Effects of global and local rewiring on SIS epidemic adaptive networks. Siam Physics Congress 2018, Pisanulok, Thailand (22-24 May 2018).